HELMHOLTZ INSTITUTE FREIBERG
FOR RESOURCE TECHNOLOGY

GERMAN - MONGOLIAN INSTITUTE
FOR RESOURCES AND TECHNOLOGY

The present work was submitted to the Faculty of Engineering

Investigations on how the froth height is influencing the flotation of ultrafine particles using the newly developed separation apparatus MultiDimFlot

Bachelor Thesis

By

Nyamjargal Erdeneduvchir

Supervisor 1 / Examiner 1	**Prof. Dr. –Ing. Thomas Hollenberg**
Supervisor 2 / Examiner 2	**Dr. Martin Rudolph**

Ulaanbaatar/Nalaikh, 2022.05.08

Statutory Declaration

Erdeneduvchir, Nyamjargal	15348169652557
Last Name, First Name	Student ID Number

I hereby affirm in lieu of an oath that I provided the submitted bachelor thesis

Investigations on how the froth height is influencing the flotation of ultrafine particles using the newly developed separation apparatus MultiDimFlot

I did not use any sources other than those stated. In case that the work is additionally submitted on a data medium, I declare that the written and the electronic form are completely identical. The work was not submitted in the same or similar form to any examination authority.

Ulaanbaatar, 05.07.2023	
Place, Date	Signature

Acknowledgement

The successful completion of this study was made possible through the collective efforts of everyone at the Helmholtz Institute Freiberg, the German-Mongolian Institute for Resource and Technology, as well as the unwavering support from my family and friends.

I would like to express my profound gratitude to Mrs. Johanna Sandbrink for her dedicated supervision, insightful discussions, and constant encouragement. I am also extremely grateful to my supervisor, Dr. Martin Rudolph, for his valuable guidance, advice, and support throughout this journey as well as Prof. Dr. –Ing. Thomas Hollenberg who provided me with numerous opportunities and supported me.

My sincere thanks go to all members of the Helmholtz Institute Freiberg who have contributed to the successful completion of my flotation experiments. I am particularly grateful to Mr. Mujahid Hussian Bhatti and Mr. Klaus Greece for their assistance and commitment during the experimental work. Additionally, I want to express my appreciation to all staff members of the German-Mongolian Institute for Resource and Technology for their support and encouragement during my undergraduate academic life.

Finally, I would like to extend special thanks to my family and friends for their unwavering support, encouragement, and belief in me throughout my academic endeavors.

Table of content

List of Figures

List of Tables

List symbol

Symbol	Unit	Description
ENT	-	Degree of entrainment
k	min^{-1}	Flotation rate constant
k_m	min^{-1}	Modified flotation rate
E_{Col}	-	Bubble-particle collection efficiency
E_C	-	Collision efficiency
E_A	-	Attachment efficiency
E_S	-	Stability efficiency
SI		Selectivity index
R_t	%	Recovery
m	kg	Mass
$R_{m,i,t}$	%	Mass recovery
t	Min	Flotation time
θ_{Young}	°	Contact angle
γ	J/m^2	Interfacial tension between two phases
ρ	kg/m^3	Density
x	µm	Particle size
X	-	Mean value

Index

C	Concentrate
cum	Cumulative
F	Feed
T	Tailings
W	Water
s	Solid phase
g	Gas phase
l	Liquid phase
G	Valuable mineral (Glass particle)
M	Gangue mineral (Magnetite)

Abbreviations

Abbreviations	Definition
CO, C6, C10	Hydrophobic states of the glass particles
CaO	Calcium oxide
Fe	Iron
Fe_2O_3	Hematite
Fe_3O_4	Magnetite
XRF	X-ray fluorescence
HCl	Hydrochloric acid
KCl	Potassium chloride
MgO	Magnesium oxide
Na_2O	Sodium oxide
PEG	Polyethylene glycol
SiO_2	Silicon oxide
Sph	Sphere (Glass particle)
Frag	Fragment (Glass particle
HIF	Helmholtz Institute in Freiberg
Al_2O_3	Aluminum oxide
C1 to C5	Froth concentrates in flotation test
GMIT	German-Mongolian Institute for Resource and Technology
T	Flotation test
DFG	German Research Foundation

1 Introduction

Flotation is a separation process that is based on differences in the surface wettability properties of materials. Hydrophobic particles adhere to air bubbles and create particle-bubble aggregates that rise in suspension and form a froth layer, whereas the hydrophilic particles sink and remain in the pulp. The flotation process is widely applied in the separation of fine particles with a particle size range between 10 µm and 200 µm. However, the flotation of ultrafine particles ($x < 10$ µm) is facing challenges and unwanted ultrafine gangue particles have a high probability of being entrained, which reduces the quality of the product.

The thesis work is conducted within one part of the MultiDimFlot project to investigate the influence of froth height on the flotation of ultrafine particles using the newly developed separation apparatus MultiDimFlot. MultiDimFlot is part of the priority program SPP 2045 MehrDimPart funded by the German research foundation. The project aims to develop a new multidimensional separation apparatus with a combination of mechanical flotation cell (high turbulence for collision between particle and bubble) and column flotation cell (fractionating effect on particle–deep froth), which separate ultrafine particles more efficiently.

The experimental work is conducted at fixed parameters (rotor speed, air rate, frother concentration) using a model feed consisting of magnetite (non-floatable) and different glass particles (floatable) with varying column lengths (column lengths of 80 cm, 60 cm). The glass particles have various shapes (fragments and spheres) and three different wettability states (hydrophilic, medium hydrophobic and highly hydrophobic). All experiment works were completed at the Department of Process at the Helmholtz-Institute Freiberg for Resource Technology from December 2022 to February 2023.

2 Literature review

2.1 Froth Flotation

Flotation is an effective method to separate valuable particles from unwanted gangue minerals with size ranges between 10 μm and 200 μm. The flotation process is based on the surface wettability characteristics of materials, but the natural characteristic of the mineral is insufficient for successful flotation separation. Therefore, additive chemical reagents, such as collectors, modifiers, and frothers, are required to manipulate the relative hydrophobicity of the particles and maintain/keep the proper froth formation.

The raw material mixtures are dispersed in the liquid phase. Hydrophobic particles attach to air bubbles and generate the bubble-particle aggregate in the suspension zone. The bubble-particle aggregates are rising to the froth zone and create a froth layer at the top of the flotation cell. Meanwhile, the hydrophilic particles settle and remain in the slurry mixture. Figure 5 shows the flotation procedure.

Many sub-processes and micro-processes (see in Table 1) take place and many factors have been investigated in flotation, which determine and influence the success and speed of the separation process.

Table 1 Schematic of sub-prpocesses in flotation (1)

The introduction of feed materials		
	Introduction of pulp	(1)
	Introduction of air	(2)
The attachment of particles to bubbles		
	Collisions between particles and bubbles	(3)
	Adhesion of particles to bubbles	(4)
	Detachment of particles from bubbles	(5)
The transport processes between pulp and froth		
	Transport of mineralized bubbles	(6)
	Direct entrainment of particles into froth	(7)
	Return of particles from froth to pulp	
The removal of flotation products		(8)
	Removal of froth	(9)
	Removal of tailings	(10)

2.1.1 Wettability

Wettability is the ability of a mineral surface to be wetted by a liquid and plays a crucial role in the effectiveness of the flotation process. There are three phases involved in froth flotation, solid phase (s), liquid (l) and gas phase (g). The drop of liquid meets a solid boundary with surrounding gas, which is called three-phase contact line at equilibrium state as shows in Figure 1. The contact angle ($\boldsymbol{\theta_{Young}}$) is a common measure of the wettability of a solid surface.

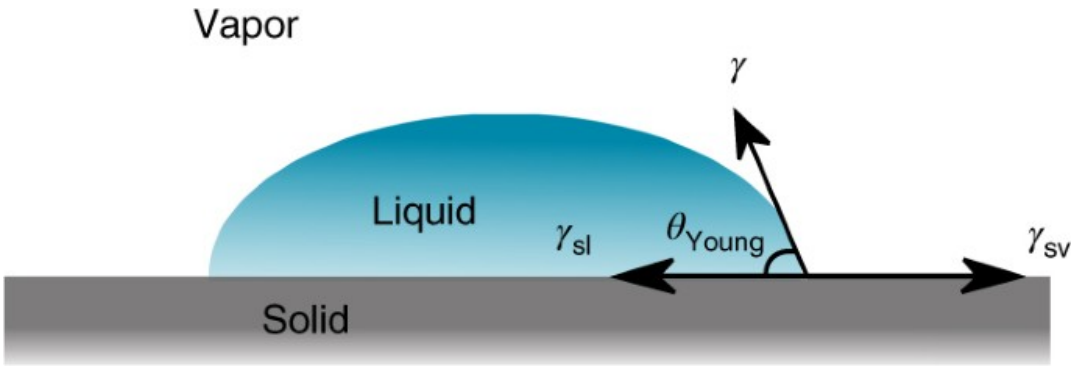

Figure 1 Schematic illustration of water droplet on solid substrate and existing parameters in Young's equation (2)

The Young's equation for contact angle $\boldsymbol{\theta_{Young}}$

Equation 1: $$\boldsymbol{\gamma_{SV} = \gamma_{SL} + \gamma * cos\ \theta_{Young}}$$

- $\boldsymbol{\gamma_{SV}}$ (solid-gas), $\boldsymbol{\gamma_{SL}}$ (solid-liquid), and $\boldsymbol{\gamma}$ (liquid-gas) - Interfacial tension
- $\boldsymbol{\theta_{Young}}$- contact angle

Equation 2: $$\boldsymbol{cos\ \theta_{Young} = \frac{\gamma_{SV} - \gamma_{SL}}{\gamma}}$$

Equation 2 only applies under following conditions:

- $\boldsymbol{\gamma_{SV} - \gamma_{SL} \leq \gamma}$
- Three phases are in equilibrium
- Solid surface is materially homogeneous
- Gravitational force is neglected

Particles with contact angles $\boldsymbol{\theta_{Young} < 90°}$ are considered hydrophilic, whereas particles with contact angles $\boldsymbol{\theta_{Young} > 90°}$ are considered hydrophobic. The larger the contact angle, the higher the adhesion between bubbles and particles in suspension as it is easier for the bubble to attach to hydrophobic particle (3).

This fundamental contact angle method is applied for homogenous, flat and smooth substrates. However, the real mineralogical particles have rough surfaces and material inhomogeneities. Therefore, other methods have to be applied to investigate the influence of the particle shape on

the wettability of the particle, such as inverse gas chromatography as presented by Sygusch & Rudolph, 2021 (4).

2.1.2 Flotation reagents

Flotation is a physicochemical interfacial separation process, which is controlled using a range of chemicals. Flotation reagents are chemical compounds that are used to enable successful separation of valuable minerals by modifying the surface properties of mineral particles. Collectors, frothers, and modifiers are three main type of reagents of flotation. Each of the reagents are utilized equal contribution and important to the separation process (3).

Collectors

Collectors are used to adsorb onto the surfaces of the selectively targeted particles. Collectors are classified and have a non-polar and polar group in their molecular structure. The non-polar collector molecule is a hydrocarbon radical, which is water-repellent and insoluble in water and rendering the surface hydrophobic by making its surface with thin film. On the other hand, the polar part can react with water. The polar part consists of large groups of anionic and cationic collectors and selectively attaches to the mineral surfaces. Collectors increase the contact angle and thus increase the hydrophobicity of the particles so that bubbles adhere to the surface better (3).

Frother

Frothers and froth zone are vital roles in flotation, as they have a large influence on the recovery and the grade of the flotation product. Frothers have several functions in froth flotation.

- Frothers enable to generate stable froth formation by reducing surface tension of the aqueous solutions.
- Frothers hinder the coalescence of bubbles and stabilize bubble size.
- Frothers stimulate the attachment of hydrophobic particle to air bubbles

Frothers are categorized according to their frother behavior at different pH values, acidic, neutral and basic. Acidic frothers have two types of acid frothers are common, namely, phenols and alkyl sulfates. Neutral frothers are a large family of frother including aliphatic alchohols and polyglycol ether (3).

Modifier

Modifiers can affect multiple factors simultaneously in the suspension zone, therefore, have numerous functions. Depending on modifier functions, it can change the pH, composition of aqueous phase and surface composition of minerals and bubbles etc.. General modifiers divided into pH control, activators and depressants (3).

- **pH Control**: Flotation is based on surface chemistry, therefore it is influenced by pH. For example the attachment of collectors to mineral surfaces can be manipulated by pH.
- **Depressants** are often used to prevent collectors from attaching onto particular mineral surfaces.
- **Activator** is supported to attach air bubbles to the surface of minerals to allow other reagents to react to it.

2.1.3 Flotation techniques

Flotation cells work by creating high speed flow of air and water into the cell, which generates turbulence in the slurry and encourages the attachment of air bubbles to hydrophobic particles. Mechanical flotation apparatus is widely used in mineral processing industry, which is operated with rotor-stator mechanism. Flotation columns, on the other hand, are designed to promote froth depth in order to improve flotation efficiency. The separation columns work with counter-current flow of air and water (5). The operation, working principle, benefits and drawbacks of the flotation apparatus are included in this section.

Mechanical flotation cell

Mechanical flotation cells are used in a variety of ways all over the world. The mechanical flotation cell consists of a vessel or tank equipped with an impeller that creates a turbulent environment in the pulp. The impeller rotates and creates a vortex, which draws air into the cell through a hollow shaft. The air is then dispersed into the pulp through the impeller blades or a dispersion plate, creating small bubbles that attach to the mineral particles (6).

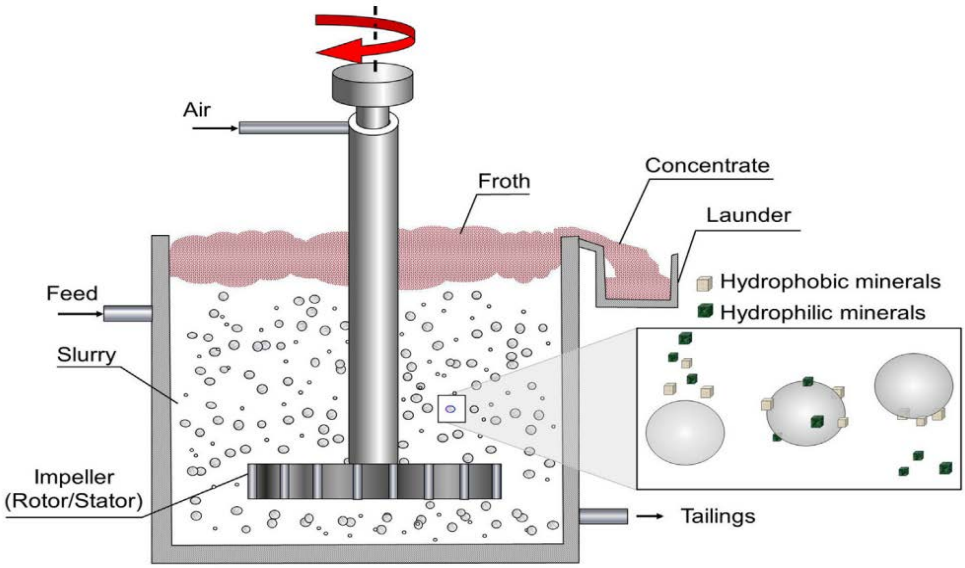

Figure 2 Principle of true flotation in a mechanical flotation cell (6)

In Figure 2, Rotor-stator mixing mechanism is at the heart of the mechanical flotation cell, which mixes the slurry, disperses air into fine bubbles (size range between 75 µm and 655 µm (7)) and creates high turbulence flow. Turbulence flow is needed to accelerate attachment between hydrophobic particles and bubbles. The bubble-particle aggregates uprise to the froth zone by buoyancy force and is removed from the cell lip.

There are essential components of a mechanical flotation cell, including cell tank, discharge box, cell launders, impeller drive assembly, impellers or rotors, stators. The cell tank design is changing and developing depending on the application. Investment and operating cost of mechanical flotation cells is higher than other cells, but the costs must be balanced against the potential benefits of improved mineral recovery and product quality.

Disadvantage of mechanical flotation cells is the relatively low froth recovery rate due to a variety of factors: size, shape of the particles, low efficiency collision between particles and bubbles, shallow froth depth. Therefore, these factors reduce product quality (6).

Flotation column

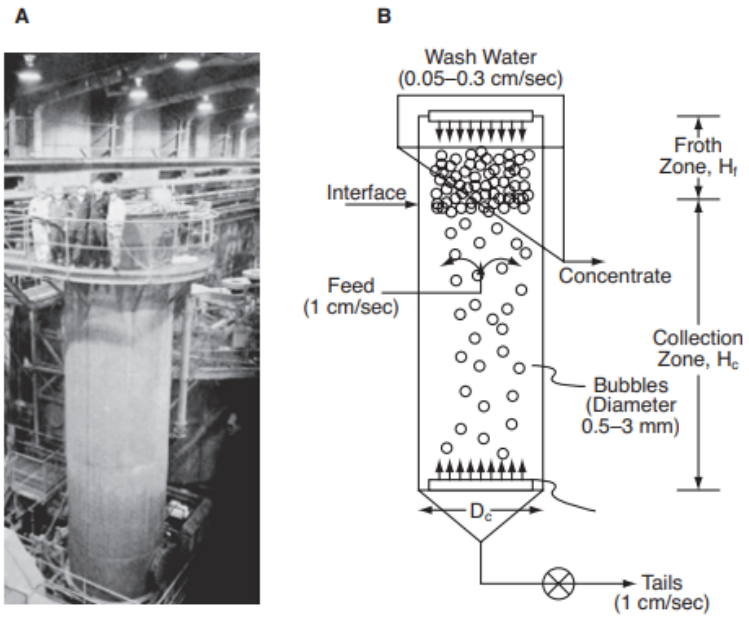

Figure 3 General schematic of conventional flotation column cell (3)

Flotation columns consists of two main zones, collection zone and the froth zone. In the collection zone, particles from the feed slurry are contacted countercurrent with bubbles created by a gas sparger (range of diameter in air bubbles is between 1 and 2 mm (8)) at the bottom of the column. In the froth zone, wash water is applied near the top of the froth for providing downward liquid flowrate, which is called positive bias. Positive bias prevents the hydraulic entrainment of the fine

particles into the concentrate. The main parameters influencing the flotation efficiency are column height (froth depth), diameter, wash water, air rate and feed solids percent (8).
There are several advantageous of flotation columns in comparison with conventional mechanical cells. Flotation column cells have lower power consumption, low capital investment and require less space in industrial scale. The cell has an ability to work with very fine particles at high solids percent while maintaining good cleaning action. Therefore, flotation column is used for cleaner flotation cell. Disadvantageous of flotation column are the high maintenance costs of, wash water costs, gas sparger maintenance and requirement of space in height. (8)

2.2 Fine particle flotation

2.2.1 Challenges

Froth flotation is a very effective separation process in optimal particle size range from 10 µm to 200 µm. The flotation kinetics and recovery Rc are reduced for ultrafine particles (x < 10 µm). Trahar and Warren (11) predicted that the poorer flotation of ultrafine is influenced by effects of sub-processes in Table 1. The influence of particle size on the flotation process has been intensively studied for a long time.

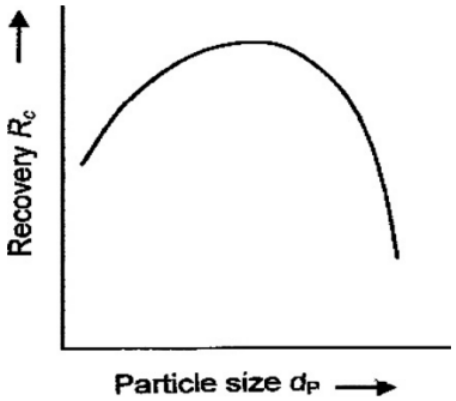

Figure 4 Recovery R_c as function of particle size d_p, schematically (11)

2.2.2 Suspension zone

The processes within the suspension zone are critical to the overall efficiency of the flotation process. To sort a mixture of particles through flotation, hydrophobic mineral attaches to air bubbles to form a stable particle-bubble aggregate that eventually reaches the froth zone. Figure 5 show that the flotation process.

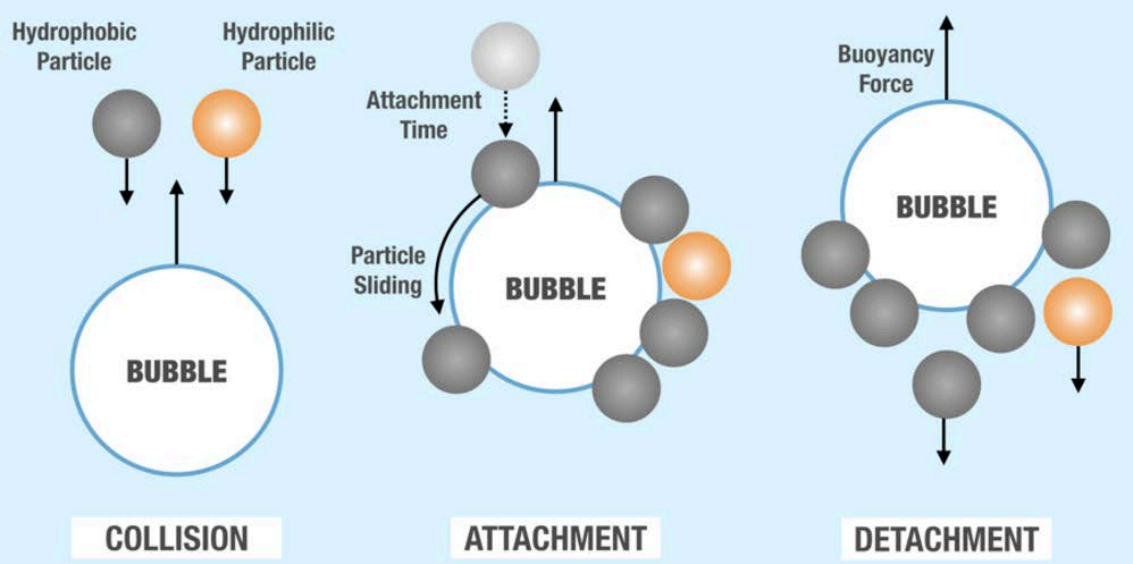

Figure 5 Flotation process (12)

The efficiency of bubble-particle collection (capture efficiency), denoted as $\boldsymbol{E_{Col}}$, can be calculated by product of bubble–particle collision efficiency ($\boldsymbol{E_C}$), attachment efficiency ($\boldsymbol{E_A}$) and stability efficiency ($\boldsymbol{E_S}$). These are independent probabilities and contribute to the overall $\boldsymbol{E_{Col}}$ (see Equation 3).

Equation 3: $$\boldsymbol{E_{Col} = E_C * E_A * E_S}$$

1. **Collision efficiency $\boldsymbol{E_C}$**

Hydrophobic fine particles (<20 μm) have a low flotation rate and recovery of hydrophobic fine particles due to their low collision efficiency, E_C with bubbles. There are several factors influencing the bubble-particle collision efficiency, including particle size and density, bubble size, bubble rising velocity and bubble surface mobility. A way to improve the bubble-particle collision efficiency is decreasing the bubble size. The decrease in the bubble size increases the bubble-particle collision efficiency and increases bubble-particle attachment efficiency (11).

2. **Attachment efficiency $\boldsymbol{E_A}$**

The process of bubble-particle attachment is complicated process, involving three stages: collision, attachment, and detachment. Collision occurs when particles encounter/come across bubbles with grazing trajectories within a range determined by the bubble diameters and particle radii. After colliding, particles slide across the bubble surfaces and may either stick to the bubbles or move away (13). Particle bubble attachment happens and a stable three-phase contact between particle bubble and liquid is formed. The bubble-particle attachment process occurs when contact time is greater than the induction time. Induction time is the duration between the

beginning of the sliding process and the initiation of attachment. The process depend on depending on the particle size, surface factors, hydrophobicity. Generally, the induction time increases with an increase of particle size, shape factors and a decrease of particle surface hydrophobicity (14).

- **Particle size**

For influence of particle size, the induction time rises with increasing particle size at constant bubble size. However, improvement of attachment efficiency can be achieved by reducing the bubble size (14).

- **Bubble size**

A decrease of bubble is increasing bubble-particles collision efficiency and attachment efficiency. However, there are certain disadvantageous for small bubbles involving the low rising velocity results in low flotation rate, very long residence time in flotation circuits. Moreover, the lifting force of small bubbles may be too low to ensure process selectivity (15).

- **Particle shape**

The effect of shape is related to micro-hydrodynamic characteristics of the particle, surface properties on the induction time and attachment efficiency was studied in (16). The particles used in this study had size ranges of 150 μm > x >106 μm and two morphologies, i.e. smooth spherical particles and ground particles (rough particle). Increasing the roughness of spherical particles results in lower induction times in bubble-particles attachment, which is studied by David et al (17). Therefore, the influence of sharp edges promotes the film rupture around bubble at the initial stage of attachment. Presence of roughness makes interaction between particle and bubbles stronger, stronger bubble-particle pairs, as well as the detachment of rough particles was lower than smooth particle. An increase of the surface roughness can enhance stability of the particle-bubble aggregate formed during flotation (16).

- **Hydrophobicity**

B. Vaziri Hassas et al. (14) observed that the hydrophobized particles where rougher hydrophobic particles had higher contact angles. The shape factors and surface wettability are evaluated together.

3. **Stability efficiency** E_S

When the three-phase contact line between bubble-particle is created, it can withstand the detachment forces. As the particle size increases, detachment forces also increase, making it more challenging to maintain stable particle-bubble aggregates. To achieve successful flotation, the particle-bubble aggregates are formed stable. Hence, if smaller particles form a three-phase contact line with a bubble, the particle-bubble aggregate formed is stable even in turbulent conditions. For ultrafine particles, the formation of aggregates are stable. Figure 6 (14) shows the relation between Stability efficiency and particle size at different values of contact angle.

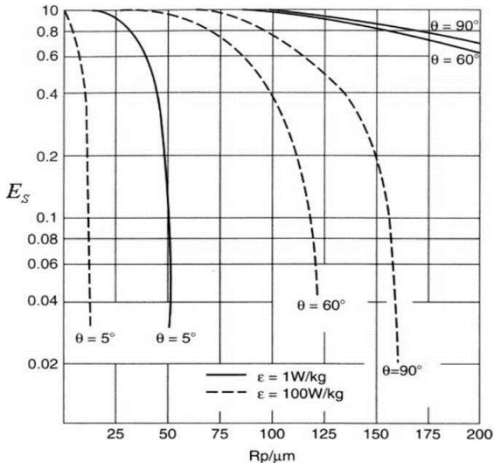

Figure 6 Relation between Stability efficiency (E_S) and particle size at different values of contact angle (13)

4. **Increase overall efficiency** E_{Col}

Reducing bubble size at constant air supply is the main way to improve collision efficiency E_C and aggregating the fine particles to optimum size for flotation**.** A decrease in bubble size also increases the attachment efficiency E_A of ultrafine particles, on the other side it is influenced by particle shapes, surface properties (16) (14).

Reduction of bubble size can be achieved by different methods, which can include mechanical (designing flotation cells, shape of the rotor and stator), physiochemical (dissolved air flotation, electro flotation) as well as the use of frother for controlling bubble size. Regarding the stability of bubble-particle, the particle-bubble aggregate is stable for ultrafine particles even in turbulent conditions (14). In practical applications, enhancing fine particle flotation can be achieved by allowing longer residence times and operating with extensive collector coverage (resulting in large contact angles) (14).

2.2.3 Froth zone

The main role of the froth phase is to provide a condition for the separation of valuable minerals attached to bubbles in the slurry. The properties of the froth significantly affect the quality of the product and recovery of valuable minerals in the concentrate. Successful flotation (true flotation) process involves hydrophobic valuable mineral particles collide with bubbles then adhere to the gas bubble and create stable particle-bubble aggregates that go upward to the froth zone.

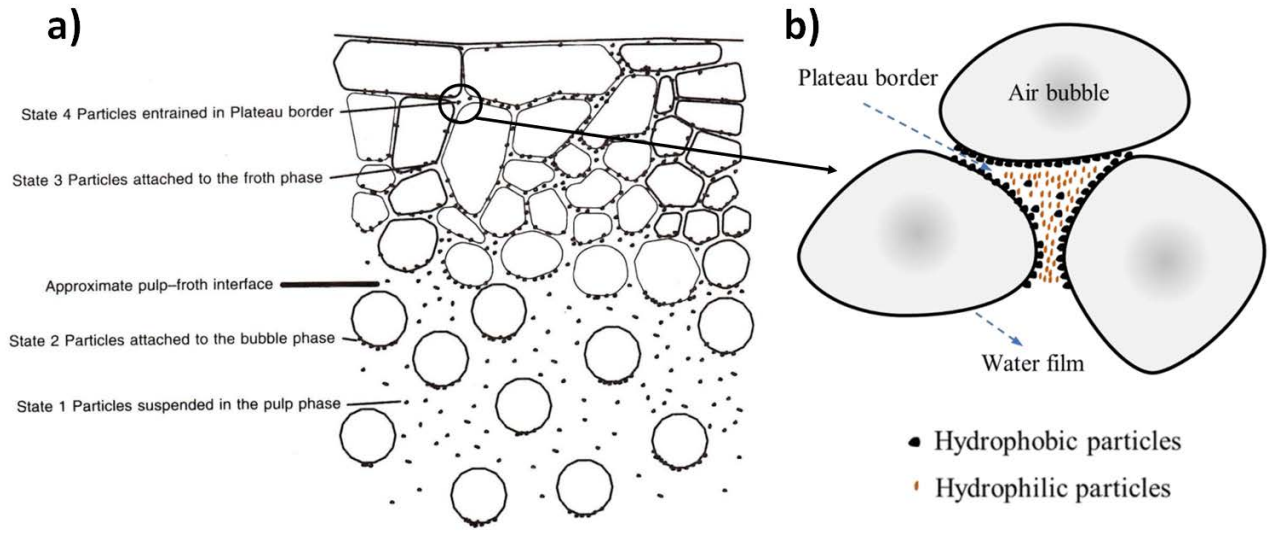

Figure 7 Recovery of the minerals during flotation process a) Location of Particles in a Flotation System (18) b) Froth lamella (19)

Three mechanisms that have been recognized as influencing particle carry froth zone: water drainage occurring in the plateau borders (the areas between bubbles), bubble coalescence, and sedimentation resulting from the relative movement of fluid and particles (18). Figure 7 (a) illustrates that particles can float in four different ways: particle suspended in the pulp zone, attachment of bubbles in the pulp zone, attached to the bubbles in the froth zone, and entrained in plateau borders. The small spherical particle-bubble aggregate (solid-laden bubble) is formed at the bottom. When aggregates rise to the froth zone, water drains downwards causing them to lose spherical shape. Then the neighboring bubbles come into contact, and the bubble coalescence occurs. Figure 7 (b) demonstrates the drainage of water in plateau borders, which is one of the mechanisms of the entrainment of particles through the froth zone (19).

In flotation, success is determined by the ability to produce the froth product that contains the maximum amount of valuable material (that can be recycled), with a high yield of the valuable material. The successful flotation process should be capable of effectively separating the valuable minerals from the gangue material and producing a concentrate with high concentration of valuable minerals.

There are two key aspects related to the froth zone.

1. Low degree of entrainment.
2. Sufficient froth stability is necessary to prevent collapse during flotation and to maintain its structure.

1. **Entrainment (ENT)**

Entrainment is a major issue in the fine particles flotation process and negatively impacts the grade of the concentrate. Numerous publications focusing on entrainment (20) (21) (22). Entrainment leads to a significant amount of the gangue materials being included in the flotation concentrates, along with the recovered valuable minerals, resulting in decreased final product quality. Typically, when the liquid flow rate of the ascending bubble-particle aggregate is greater than the settling velocity of hydrophilic particles, these particles will be undesirably captured within the froth concentrate. Entrainment is influenced by several factors in both suspension and froth zones, including particle properties (particle size and density) and flotation operational variables (air flow rate, froth depth, rotor speed, and reagent dosage).

Entrainment includes two steps. The first step involves the movement of suspended solids from the upper region of the pulp, located just below the pulp-froth interface, to the froth. The second step involves the transfer of particles, which have been entrained in the froth, to the concentrate (22).

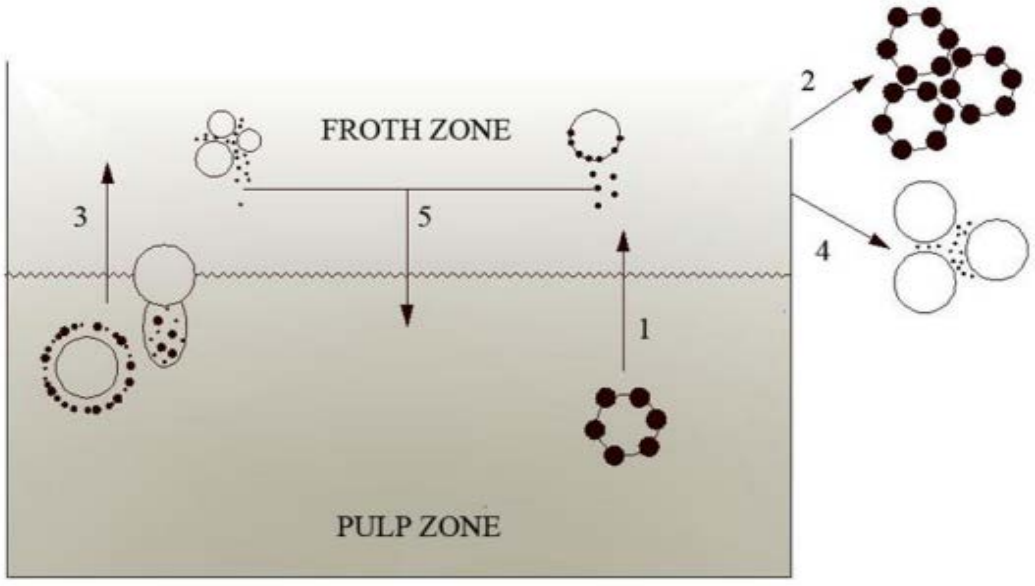

Figure 8 Mechanisms of transfer of fully liberated mineral particles in a flotation cell (20)

Mechanisms of mass transfer of fully liberated mineral particles in flotation in Figure 8

- *Process (1)* and *(2)* are the primary mechanisms targeted in flotation, where the air bubbles carrying the valuable substances are transferred from the suspension zone to the froth zone and recovered as froth concentrate.
- *Process (3)* represents the entrainment of fine particles and water (or air bubbles) are transferred from suspension to the froth zone.

- *Process (4)* shows that small particles (ultrafine particles) have a high tendency to be discharged with water into the concentrate.
- *Process (5)* depicts that the detachment and entrainment of mineral particles in the froth results in their transfer back to the pulp. This may be two side effects for flotation if the particle

Particle size

The degree of entrainment is highly influenced by the particle size, as the entrainment decreases with increasing particle size. It indicates that coarse particles tend to be less entrained to the concentrate. As can be seen in the left side of Figure 9, relationship between the degrees of entrainment and particle size (20) (22).

Particle density

Particle density also has a vital impact on the entrainment factor. Low-density minerals had a higher tendency to move with water because of their slower sedimentation velocities, as a result, they have a higher level of entrainment. Figure 9 on the right side illustrates the density impact on entrainment, using silica (SG=2.6) and galena (SG=7.5) (20).

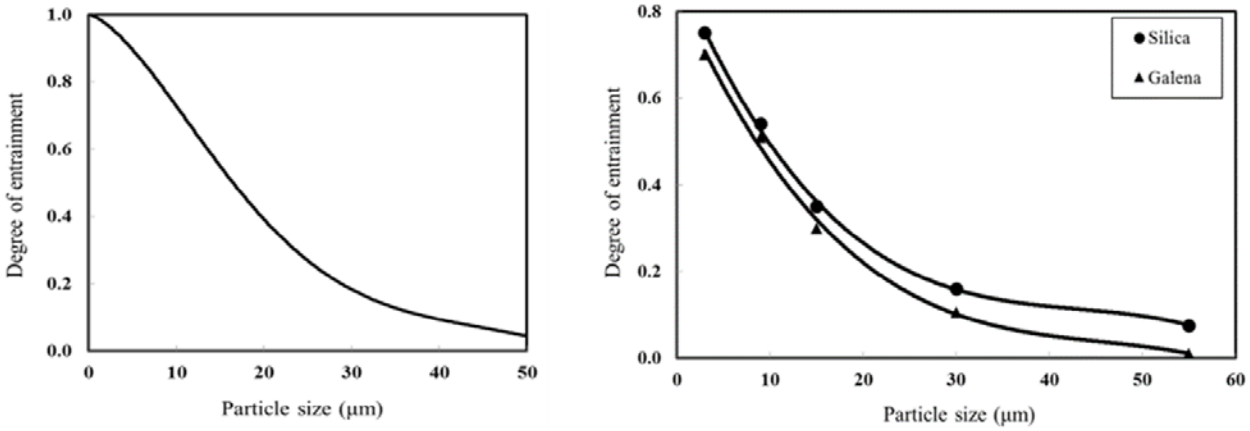

Figure 9. Left: Relationship between degree of entrainment and particle size for hydrophilic silica. Right: Effect of particle density of entrainment, silica (SG=2.6) and galena (SG=7.5) in laboratory column (20)

Particle shape

J.G. Wiese et.al (22) investigate the role of particle shape, and particle size behavior on entrainment factor in a laboratory scale. The non-spherical grain shape (needle-shaped) particles have a higher degree of entrainment than similar size range (x<25 μm) spherical particles, even though the non-spherical particles are much denser (22). The influences of different shapes, and sizes may have on the behavior of the froth.

Little et.al (23) investigated the effect of particle shape on entrainment in plant scale. The plant scale study shows that more rounded particles (25 μm > x >10 μm) have a higher tendency to

entrainment than non-spherical (angular, elongated particles). The study results are not expected and show contradictory results to the previous study.

Impeller speed/Rotor speed

Increasing rotor speed results in reduced bubble size, which also increases the probability of bubble-particle collisions in the suspension zone. It also enhances the water recovery, which results in a higher solid concentration in the pulp water moving into the froth and hence the concentrate. Consequently, more gangue minerals are entrained into the concentrate. Consequently, more gangue minerals are entrained into the concentrate (20).

Gas flowrate/Air supply

Gas flow rate is a crucial role in entrainment by influencing the water recovery into the concentrate and concentration of suspended solid particles in the water phase. When the gas flow rate is increased, more water carrying the suspended solid particles will be transferred from the pulp to the froth. Consequently, a rise in gas flow rate will lead to an increase in water recovery and in an increase in the degree of entrainment (20) in Figure 10.

Froth height

There are other parameters that affect the degree of entrainment, such as the froth height as shown by X. Zheng, *et al.* (21). The height of the froth was reduced, resulting in a wetter froth that contained more water and suspended gangue mineral particles that were transferred into the concentrate. Froth height is also a primary influencing factor for residence time. An increase in froth height leads to a longer froth residence time, allowing drainage of water and solid particles, which results in a decrease in the degree of entrainment. The right side of Figure 10 illustrates the relationship between the degree of entrainment of three selected particle sizes and froth height at the same gas flow rate.

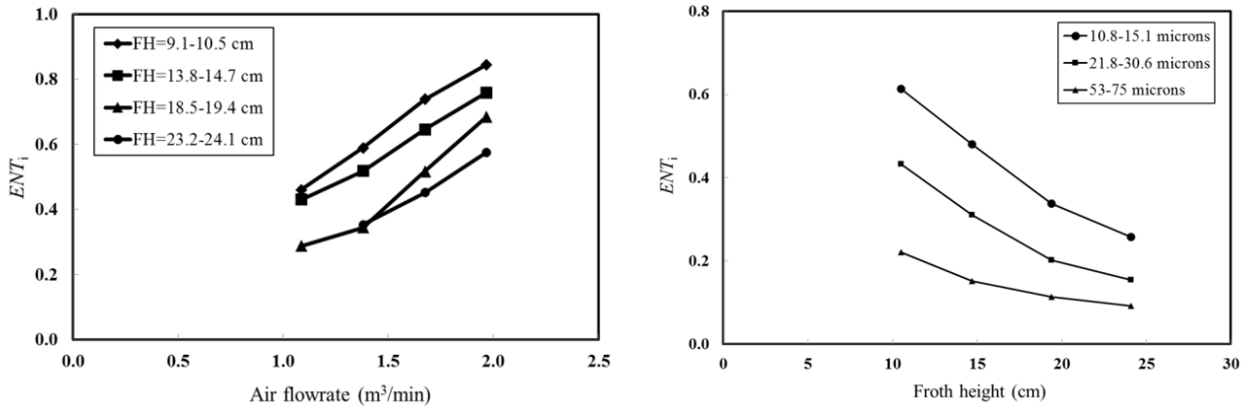

Figure 10 Left: Effect of gas flowrate on degree of entrainment (x>5.3 µm) at different froth height, Right: The degree of entrainment.

1. Froth stability

Froth stability is an indicator of froth recovery. To achieve the highest possible recovery and recyclable content in the concentrate, the froth should be dehydrated without allowing the air bubbles to collapse before being recovered as froth concentrate. The concentration and composition of frother affect the behavior of bubbles, including size, stability, coalescence tendency ,etc. As lamellar liquid drains, particles may form a bridge between loaded air bubbles, preventing the liquid film from cracking between them. The hydrophobicity, size, and shape of particles, as well as the concentration and composition of frother also influence the froth stability.

Hydrophobicity

The hydrophobicity of the particles has a high impact on the froth stability. The wettability is characterized by contact angle ($\boldsymbol{\theta_{Young}}$).

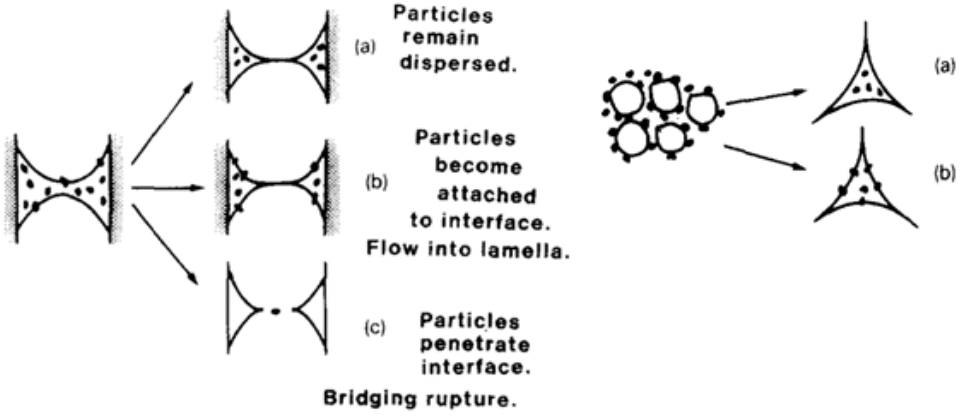

Figure 11 Stabilization and de-stabilization mechanism of the mineralized froths (a) Low degree of hydrophobicity (θ <40°), (b) Intermediate degree of hydrophobicity ((θ =65°) and (c) High degree of hydrophobicity ((θ>80°) (24)

Figure 11 depicts the impact of contact angle on particles (size range between 26 - 44 µm) to stabilize and destabilize the mechanism of the froths by bridging – dewetting mechanisms.

(a) Low degree of hydrophobicity (θ_{Young}= 40°), particles are dispersed in the liquid film/lamella phase and have little influence on the froth stability.

(b) Moderate degree of hydrophobicity (θ_{Young}= 65°), particles become attached to the interface, which enhances the rigidity of the froth structure and creates stable films and flows into lamella. Maximum froth stability may be achieved using moderately hydrophobic particles as highly hydrophobic particles tend to destabilize the froth by promoting coalescence.

(c) High degree of hydrophobicity (θ_{Young}> 80°), particles can penetrate the air/solutions interface more significantly and, prevent from streaming out during drainage. Consequently, the bubble rupture occurred as particles bridge the film, leading to destabilization (24). A High degree of

hydrophobic particles, froth destabilization, and aggregation occurred with particles forming clusters, which were harder to recover from the poor froth layer, resulting in lower flotation rates (25).

Particle shape

Particle shape is another main influencing factor on froth stability. Rougher surface particles generally have higher flotation rates than spherical particles, resulting faster rate of film thinning and rupture at rough surfaces P.T.L. Koh et al (25) and Johansson and Pugh (24) concluded that non-spherical particles have a more destabilizing impact than spherical particles.

Particle size

The froth is very stable and carried out high amounts of water and solid particles in fine particle flotation. Conversely, the coarse particles created unstable froths with larger bubbles. Also, large particles ruptured films faster. Larger particles cause films to rupture more quickly because they require less film thinning before the particle can span the film, leading to the convergence of the three-phase boundary lines at a single point (26).

3 Material and methods

3.1 Material

The ultrafine particle system is a combination of hydrophilic particles as magnetite and glass particles. The glass particles have various grain shapes, and different hydrophobic levels, which are adjusted by esterification with alcohols of different carbon chain lengths (C-chains). The characteristics of six particles shows in Table 2.

Table 2 Overall used six glass particle systems with their different particle shapes, carbon chain lengths and alcohols used esterification of particles, as well as their levels of hydrophobicity.

Particle shape	Alcohol	C-chain	Hydrophobic state
Sphere	-	C_0	none
	1-Hexanol	C_6	medium
	1-Decanol	C_{10}	high
Fragments	-	C_0	none
	1-Hexanol	C_6	medium
	1-Decanol	C_{10}	high

The feed material (mA=100 g) is prepared from the pure components of magnetite and glass in the ratio of 90 and 10 weight percent. The particle size distributions of magnetite, glass spheres and fragments by laser diffraction are illustrated in Table 3.

Table 3: Particle size distribution of the magnetite, glass spheres and fragments analyzed by laser diffraction.

	Magnetite	Spheres	Fragments
d10 in µm	0.74	0.62	0.77
d50 in µm	2.52	2.67	3.3
d90 in µm	6.69	4.99	7.55

The hydrophilic gangue mineral is magnetite (p_M=5200 kg/m^3), which was originally produced by Kremer Pigmente, Germany (27). The magnetite can be regarded as pure based on X-ray diffraction analysis.

Glass particles (ρ_G = 2500 kg/m3) with different shapes are used as valuable minerals. The spherical and fragmented glass particles are made of soda-lime glass and are products of VELOX, Germany and both have the same chemical composition of 70-75% SiO_2, 12-15% Na_2O, and 7-12% CaO, 0-5% MgO and others. The fragments were produced by air classification after milling the coarse fraction SG3000 to produce a fraction with a maximum particle size of 10 µm. The spheres were purchased as a size fraction below 10 µm (SG7010) (4). Figure 12 presented the scanning microscope images (SEM) of the used particle system (magnetite, fragment, spheres).

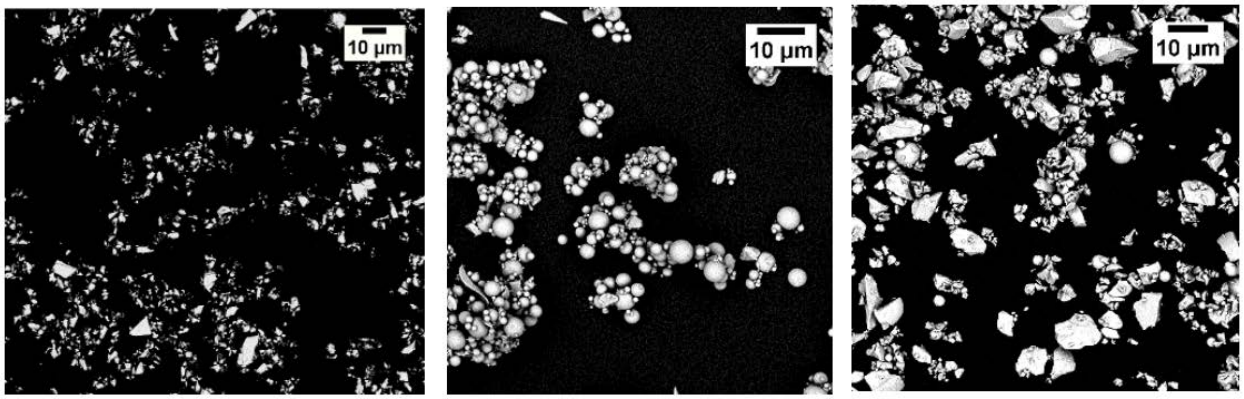

Figure 12 SEM images of the used particles system: magnetite, glass spheres, glass fragments (from left to right) (27)

The surface wettability of the glass particles is changed by esterification with alcohols, straight-chain alcohols 1-Hexanol, and 1-Decanol, which are used. The esterification reaction between the hydroxyl groups of the alcohol and the silanol groups on the surface of the glass particles results in a chemical attachment of the alkyl chains through ether bonds onto the particle surface by condensation (4). The following reactions are shown in Figure 13.

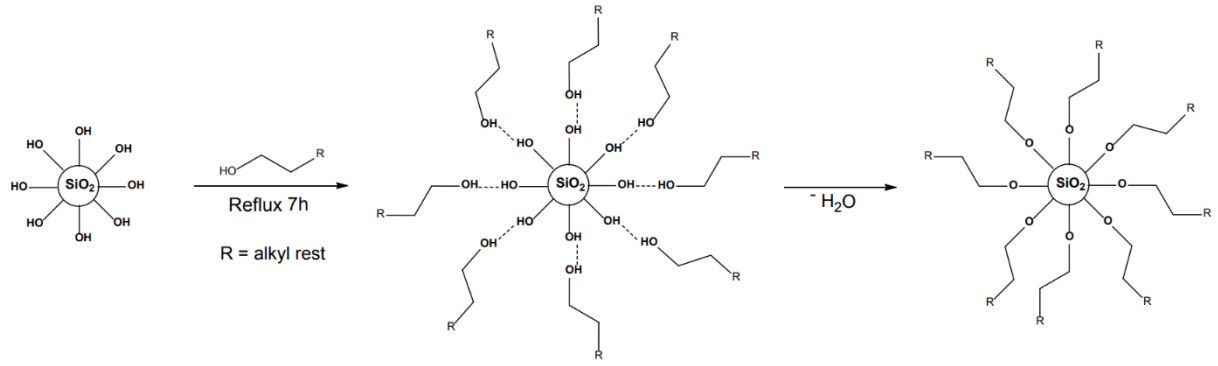

Figure 13 the general schematic representation of esterification of glass particles (4)

The wettability analysis uses analytical techniques such as static and dynamic contact angle measurement, analytic particle solvent extraction, and inverse gas chromatography (IGC). which

was not part of the current study, but was investigated prior by Sygusch & Rudolph, 2021 (4). Those measurements help to see an extended view of particle wetting characteristics like how the particle properties of size and shape are affected the wetting behavior.

Figure 14 shows that the values of contact angle increase as the number of carbon atoms (used for the esterification reaction, e.g. from particles esterified with 1-Hexanol C6 to particles esterified with 1-Decanol C10) increase, which indicates more hydrophobic materials or the materials' wettability is reduced. The contact angle measurement supports a determination of the variety of surface heterogeneity, but esterification utilizing long-chain alcohols reduces contact angle hysteresis, making the surface more homogeneous.

IGC is a sensitive analytical approach capable of identifying energetic differences by specific surface free energy parameters, which neither static nor dynamic contact angle measurements can identify. For the study, the materials were analyzed via inverse gas chromatography (IGC) which showed that longer alkyl chains could cover larger parts of the surface, which consequently decreases the surface energy. On the other hand, shorter alkyl chain length can only partially reduce some highly energetic surface sites, which might still not be sufficient to affect the resulting surface energy. As far as the contact angle measurement is supported to make results but it is not enough to functionalize completely the results.

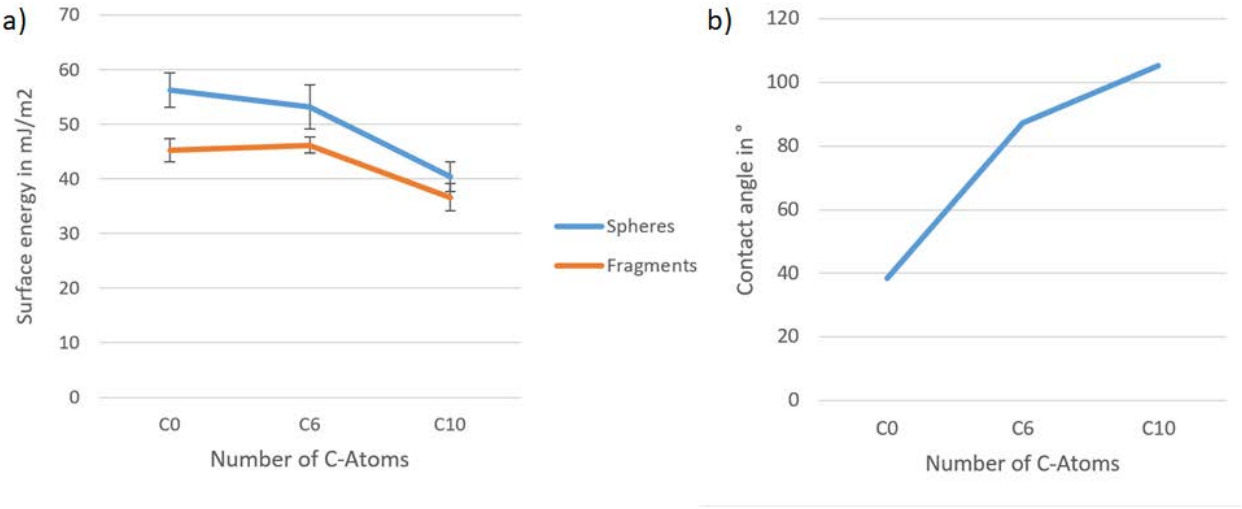

Figure 14 a) Measurement results of specific surface free energy in glass particles b) Contact angle measurement results on soda lime glass particles (4)

After analyzing the methods, it is shown the fragments generally have a lower specific surface free energy and thus higher hydrophobicity than the spheres, even with the same chemical composition. Generally, the wettability of the functionalized particles can be controlled by the esterifying alcohol, which means longer alkyl chains result in producing more hydrophobic particles with more homogenous wettability features.

The liquid phase

Polyethylene glycol ($OH(C_2H_4O)_nH$) is used as a frother at a concentration of 10^{-5} M for all flotation tests, chemical structure of the compound is shown in Figure 15. The substance is a solid polymer with an average molar mass of 9000-11250 g/mol. Polyethylene glycol is characterized by a high solubility in water (500 g/l at 20 °C).

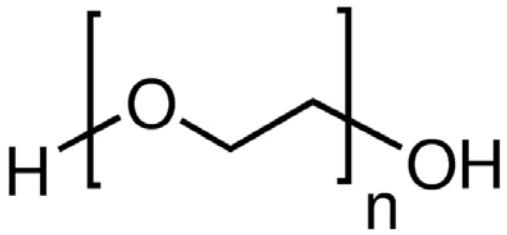

Figure 15 Structure of polyethylene glycol (28)

For flotation a PEG-solution of 10^{-5}M is used, which is prepared by dissolving the PEG in a 10^{-2} M KCl solution in deionized water (29).

3.2 Methods

3.2.1 The MultiDimFlot apparatus

Flotation apparatus

All flotation experiments are performed with the newly designed MultiDimFlot flotation apparatus. The flotation apparatus consistS of a bottom-driven Magotteaux conventional mechanical cell combined with flotation columns. Figure 16 (c) shows the rotor speed and air supply regulator of the flotation machine. The air supply is controlled by a Bronkhorst air flow meter and the maximum capacity is 1 l/min. The rotor stator system is a maximum rotor speed of 1380 min^{-1} and is operated at the main bottom of the flotation cell.

The flotation columns used in this study have a length of 40 cm, 60 cm, and 80 cm. In a previous study of MultiDimFlot, the experiments are done at a fixed column length of 100 cm in all tests. (a) shows the available columns. Each of the columns has 5 cm internal diameter.

The Magotteaux cell is shown in Figure 16 (b), which has an inlet hosepipe of the Ismatec Ecoline pump and an outlet for removing tailings after the flotation test. The concentrate is removed with a paddle and the water level in the suspension zone is decreased during the experiment. Hence, additional deionized water is required to keep the water level by the Ismatec Ecoline pump. The

pump has a thick hosepipe, which is adjustable with a two-digit potentiometer, whereby a flowrate between 1.6 to 5000 mL/min per channel.

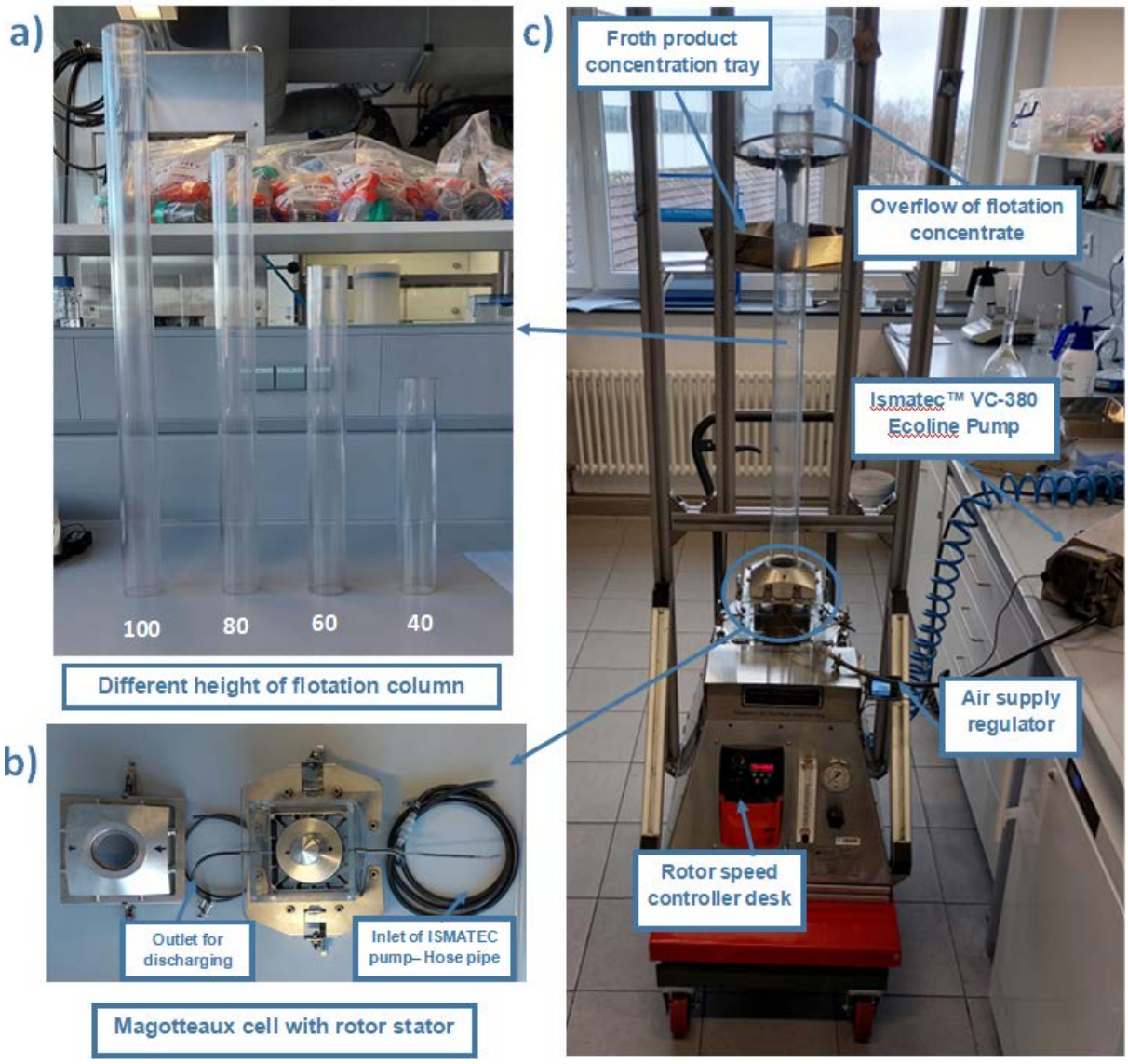

Figure 16 a) Different height of flotation columns b) Picture of Magotteaux cell with rotor-stator (Outlet – Inlet) c) MultiDimFlot separation apparatus

Figure 21 (a) shows a schematic representation of the MultiDimFlot flotation apparatus, and the practical MultiDimFlot flotation apparatus is illustrated in Figure 21 (b).

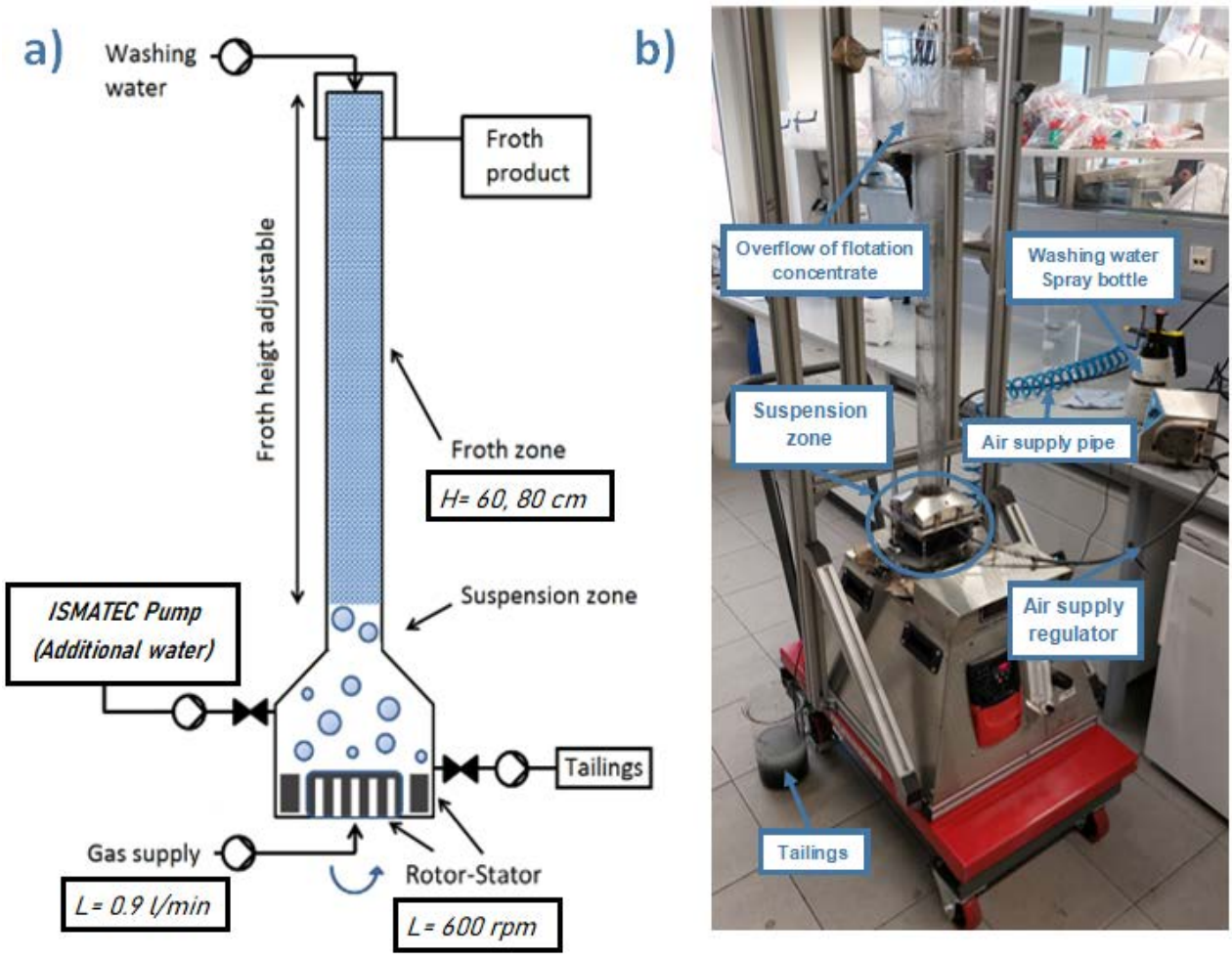

Figure 17 a) Schematic representation of MultiDimFlot separation apparatus b) The main part description of MultiDimFlot apparatus

3.2.2 Flotation

Preparation

Each flotation test includes the preparation, main flotation, and post-processing parts. The first step is the preparation of the feed liquid suspension because the frother PEG needs some time to dissolve. For this purpose, 0.2 g of the frothier PEG is dissolved in 2-liter of a 10^{-2} mol/l KCl background solution. The solution is stirred on a magnetic plate with a magnetic stirrer until the PEG is completely dissolved. The feed solid suspension should have a content of 90% of magnetite (90 g) and 10% of one glass particle fraction (10 g), i.e. either spheres or fragments. The weighted solid particles are mixed with feed solution and then dispersed with the ULTRA-TURRAX disperser (IKA, Germany, dispersing tool S25N-25F) at a rotational speed of 11,000 min-1 for 1 minute. After dispersing the particles, the suspension was transferred to the flotation

cell using funnels. Meanwhile, the Magotteaux cell rotor is already operating at a low speed to avoid solid phase settling.

Flotation test

The rotor speed and air supply are set with fixed optimum parameters at 600 rpm and 0.9 l/min. The time for the froth to build up in the column is noted. Once an overflow of the froth out of the column is observed the flotation test begins. In a previous Bachelor study, these parameter settings have been found to be most suitable for this particle system (30). Every 10 seconds, the overflow is mechanically removed with a paddle and fed to the froth collection area. At defined time intervals, the concentrate between C1 to C5 is removed from the flotation process into the concentration tank. The concentrate is collected after 1 min (C1) – 2 min (C2) – 4 min (C3) – 6 min (C4) – 8 min (C5). The concentration tray and spray bottle are weighted after each concentration. Five concentrates are collected after full flotation processes within 8 min flotation, and the rotor and air supply are stopped when flotation is done. If the froth is collapsing and no overflow is observed within t<8 min, the air supply is switched off and the flotation time is noted. Additionally, the collapsing time of the froth is measured after switching off the airflow meter. After collapsing of the froth, the rest of the product in a flotation cell is transferred into the tailing beaker via the drain hose. Each concentrate tray, used spray bottle water, and tailing beaker must be weighed.

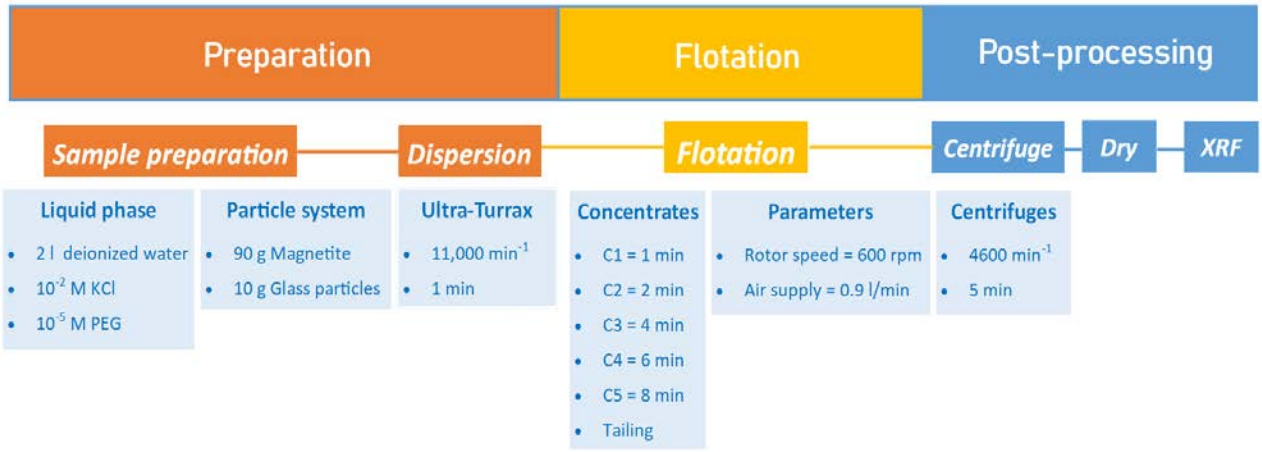

Figure 18 Experiment procedure of flotation test in MultiDimFlot separation apparatus

Post-processing

Afterward, the post-processing of the flotation experiment begins. Both the tailing and concentrated products are dewatered using a centrifuge at 4600 min^{-1} for 5 min. The products are

filled into separate centrifuge containers. To prevent imbalances, it is crucial to balance the weight of the containers. Deionized water should be added if necessary to adjust the weight. After centrifugation, the remaining solid phase is transferred to a beaker with as little deionized water as possible and dried in a drying oven at 80 C until fully dried. The sample is weighted and transferred to a sample container for X-ray fluorescence analysis when the mass is constant. When weighing the sample, it must be necessary to weigh beakers in advance, both the particle mass and water mass of concentrates or the tailing product can be collected.

3.2.3 Experimental plan

The main purpose of the study is to investigate the influence of the froth height on the separation outcome and how the particle properties (wettability level and morphology) affect the fractionating characteristics within the froth.

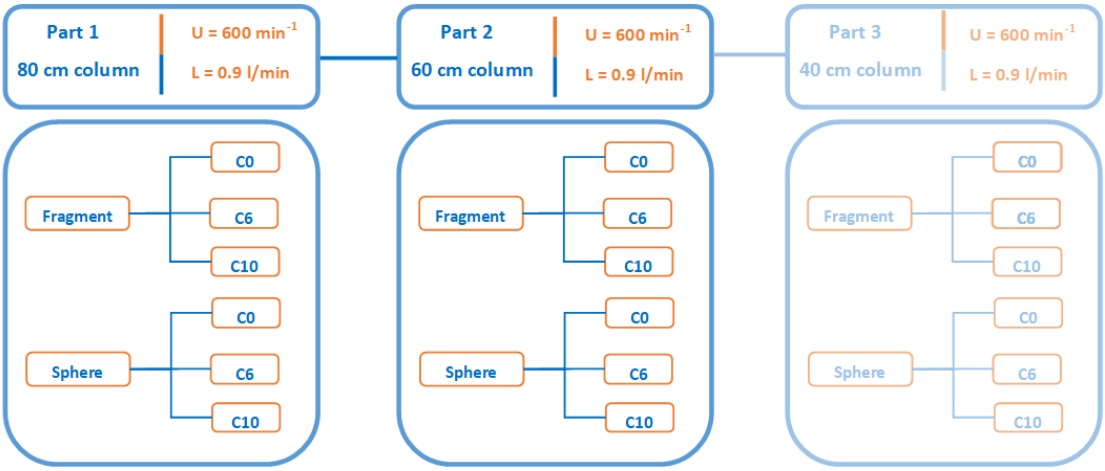

Figure 19 The experiment plan consists of three different column heights in 40, 60, and 80 cm columns at 600 rpm and 0.9 l/min of fixed parameters.

We planned to do 54-flotation experiments with three different column heights of 80 cm, 60 cm, and 40 cm in Figure 19. These column heights correspond to different parts of the column. We used a model feed comprising magnetite and glass particle fractions. In the experiment, we used six glass particles with various shapes and hydrophobicities (see Table 2) to investigate the effect of particle shape and hydrophobicity at different column heights on the flotation process. All flotation tests are accomplished at fixed operating parameters (rotor speed at 600 rpm, air rate at 0.9 l/min), which values were found by Nora Stefenelli, a previous bachelor's thesis student in the MultiDimFlot project. However, a flotation test at a 40 cm column is not possible due to the low froth height.

3.2.4 X-ray fluorescence analysis

Functional Principle

XRF (X-ray fluorescence spectroscopy) analysis is a non-destructive method for quantitative and qualitative determination of the elemental composition of solids, liquids as well as powders. X-radiation penetrates the specimen, hitting an electron of an atom close to the nucleus and knocking it out of the electron shell. This results in an electron vacancy in the inner shell, which is occupied by an electron from a higher shell. The transitions between different electron levels result in X-ray fluorescence radiation. The energy level varies depending on the type of emitting atom, this radiation is called characteristic radiation. If the sample comprises several elements, the fluorescence radiation of the element has the largest measuring effect with a large number of fluorescence energies of different intensities. The energy dispersive detector measures the energy distribution of fluorescence radiation. This measured spectrum shows lines or peaks that are characteristic of the chemical elements in the sample. Figure 20 depicts the schematic configuration of the XRF analyzer.

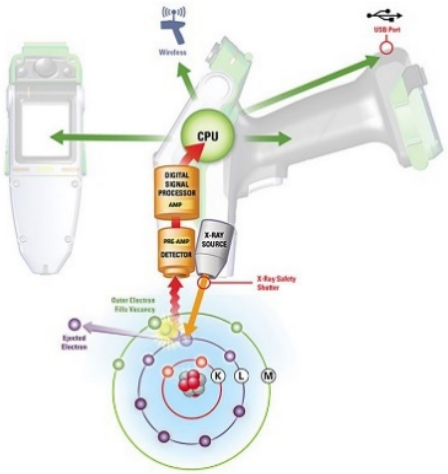

Figure 20 Schematic configuration of hand-held XRF analyzer (32)

Figure 21 S1 Interlocked Benchtop *stand (Left), S1 TITAN Handheld XRF Analyzer (Right) (31)*

S1 TITAN Handheld XRF Analyzer

In our experiment, S1 TITAN Handheld XRF Analyzer from BRUKER is used to analyze the sample. Figure 21 shows the accessories of the XRF analyzer, including a USB cable, AC adapter, and an interlocked Benchtop stand, which directly measures the bags, and pellets. The interlocked Benchtop stand provides the XRF analyzer to analyze the horizontal sample and can connect to the extension pole. Moreover, the analyzer is a transportable and great choice for analyzing heavier elements beginning with sulfur. The device's elemental range is between Mg and U (31).

Procedure

At first, the dried powdery sample material is filled into a plastic sample container, which is covered with standard household food plastic wrap. For a true analysis result, the plastic wrap should not wrinkle. It would affect the XRF analysis if it was wrinkled. A plastic film covers the container within an interlocked Benchtop stand and the surface faces downwards over the X-ray diffraction device. The sample is placed in the container, the lid is closed, and then the measurement begins. The device can detect heavy elements such as iron, copper, zinc ,etc. Three XRF analyses are performed for each sample. The plastic container is shaken by hand in between each particular sample measurement, and the mean value is calculated at the end.

XRF is used to measure the proportion of elemental iron in the sample. The software used for data analysis is called GeoChem, which only outputs the proportion of Fe_2O_3 ($C_{Fe_2O_3}$ in wt. %) in mass percent as the analysis value when GeoChem General Calibration is used. The measurement result is calibrated with hematite (Fe_2O_3) at the end, the iron content is 70 wt. %. Due to this difficulty, conversion of the hematite content ($C_{Fe_2O_3}$) determined by GeoChem must be converted to magnetite content ($C_{Fe_3O_4}$) by following the two-step equations below.

Table 4 Molecular weight of Fe, Fe_2O_3 and Fe_3O_4 (32)

Name	Formula	Molecular weight (MW) in g/mol
Iron	Fe	55.845
Hematite	Fe_2O_3	159.688
Magnetite	Fe_3O_4	231.533

Equation 4: $$\mathrm{C_{Fe}} = \mathrm{C_{Fe2O3}} * \frac{2 * \mathrm{MW_{Fe}}}{\mathrm{MW_{Fe2O3}}} \quad \textit{in wt. \%}$$

Equation 5: $$C_{Fe3O4} = c_v = C_{Fe} * \frac{MW_{Fe3O4}}{3 * MW_{Fe}} \quad \textit{in wt. \%}$$

The content of waste mineral (c_W) is calculated in following equation:

Equation 6: $$c_W = 100\% - c_v \text{ in wt. \%}$$

The iron content of pure magnetite is 72 wt. %. This value cannot be determined using the S1 TITAN instrument and the current GeoChem General calibration. Therefore, it is necessary to refer to the particle system under investigation in order to obtain this information.

3.2.5 Evaluation of the separation process

Three material mass flows and their recyclable material contents are measured in the flotation process.

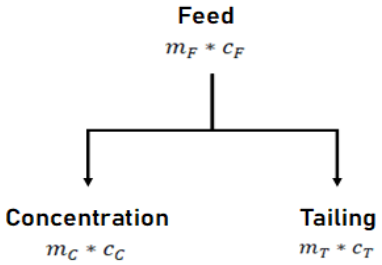

Figure 22 Schematic configuration of material flows of a flotation process with masses m and the recyclable material content

Equation 7: $$m_F = m_C + m_T$$

Equation 8: $$m_F * c_F = m_C * c_C + m_T * c_T$$

m_F is the feed into the flotation process, which is sum of concentration mass (m_C) and mass of tailings (m_T). Taking into account the material content, (c_F) in the material flow. The mass balance is formulated

Mass recovery

Mass recovery ($R_{m,i,t}$) is calculated as the proportion of the mass of flotation products to the mass of the flotation feed for a specific size (i) and flotation time(t).

Equation 9: $$R_{m,i,t} = \frac{m_{i,t}}{m_{total}}$$

Recovery

The overall recovery was calculated from the mass-balanced stream flows (feed, concentrate, and tailings) for desired particle classes, unsized mineral flow, size-by-mineral or size-by-liberation mineral flow in Equation 10

Equation 10: $$R_{i,t}^{x} = \frac{m_{i,t}^{x}}{\sum m_i^x}$$

Here, $\sum m_i^x$ is mass of mineral (x) of the interest in the feed for size(i).

Water recovery

Water recovery (R_W) is determined as fraction of water recovered in concentrate to the water added to the flotation cell.

Equation 11: $$R_W = \frac{m_{W,t}}{m_{W,pulp}}$$

Here, $m_{W,t}$ is the mass of water in the concentrate product at time(t), as well as $m_{W,pulp}$ is the mass of water in pulp.

Mineral grade

The grade of the desired mineral x is determined by the computing the ration of mineral x's mass to the overall mass of the ore sample.

Equation 12: $$c_{i,j,t}^{x} = \frac{m_{i,t}^{x}}{m_{i,t}}$$

Here, $m_{i,j}^{x}$ represents the mass of mineral (x) of interest of size (i) and flotation time (t).

Flotation kinetics

The classical first order kinetic model is generally used as a flotation kinetic model to evaluate the effects of variables on flotation. $R_{\ t}$ is the cumulative recovery at time t, $R_{\ max}$ is cumulative maximum recovery and k is the flotation rate constant (9).

Equation 13: $$R_{\ t} = R_{\ max}(1 - e^{-kt})$$

To compare the flotation kinetics of different particle systems or the influence of certain operating parameters, the modified flotation rate constant km is calculated.

Equation 14: $$k_{\ m} = R_{\ max} * k$$

Evaluation of flotation performance

Equation 15: $$SI = \sqrt{\frac{R_C*(100-R_T)}{(100-R_C)*R_T}}$$

To evaluate the effectiveness of separating gangue minerals from valuable minerals, the selectivity index SI value is comprehensive evaluation metric, with a range between zero and infinity. A high selectivity index is the goal of the separation process, as this indicates a successful transfer of the valuable substance into concentrate with little to no recovery of gangue minerals.

Entrainment

The degree of entrainment (ENT) is determined by the ratio of the mass of gangue mineral per unit mass of water in concentrate and mass of gangue mineral per unit mass of water in tailings.

Equation 16: $$ENT = \frac{(Mass\ of\ free\ gangue\ per\ unit\ mass\ of\ water\ )_{concentrate}}{(Mass\ of\ free\ gangue\ per\ unit\ mass\ of\ water\ )_{tailings}}$$

The degree of entrainment (ENT) value is between zero and one. The goal of the flotation is $(ENT \to 0)$.

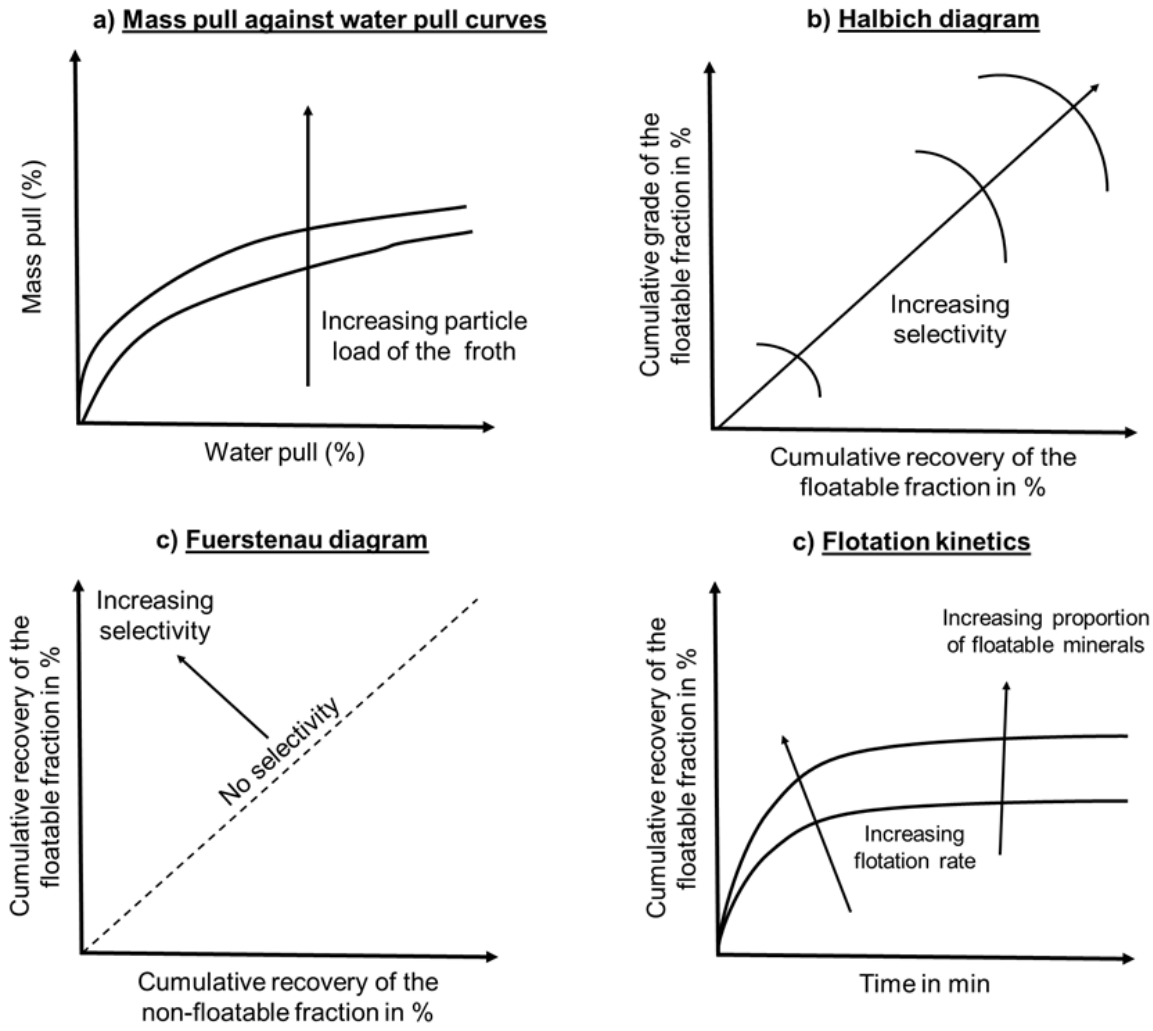

Figure 23 Evaluation diagrams for success of flotation a) Mass VS Water pull curve b) Halbich diagram c) Fuerstenau diagram d) Flotation kinetics (10)

Several diagrams can assess the success of the separation process in Figure 23

a) **Mass pull versus water pull diagrams** provide an indication on the quality of the froth and its particle load.
b) **Halbich curves** enable the comparison between different flotation runs, and gives a relative idea of the maximum selectivity achieved based on the chosen parameters.

c) **Fuerstenau diagram** is also a selectivity curve, indicating that the recovery of the valuable mineral should be significantly higher than that of the gangue. Ideally, curves should be located as far left and above 45 degrees “no selectivity” line as possible.
d) **Flotation kinetics** indicates the proportion of floatable mineral, while the slope of the curve gives information about the rate of flotation recovery.

These diagrams can help in evaluating the separation process’s success and understanding the performance of different flotation parameters (10).

4 Results and discussion

In the discussion section, we will analyze the outcomes from 40 flotation tests carried out with the MultiDimFlot apparatus. The experiments were conducted in fixed parameters (rotor speed at 600 rpm and air rate at 0.9 l/min) and involved six different particle systems at column heights of 60 and 80 cm. In addition, we also consider the results at 100 cm column height by Nora Stefenelli (30), who is a previous bachelor thesis student in part of MultiDimFlot project. The discussion part recover the investigation of froth height impact on the flotation of ultrafine particles by comparing the obtained at different column lengths (60, 80, and 100 cm). Furthermore, we explore the influence of particle properties, including wettability state and morphology, on flotation performance as observers in the experimental results.

4.1 Influence of particle shape with constant wettability state at different column heights

Fragment/ Sphere C0:

FragC0 and SphC0 are hydrophilic particles and are unesterified with alcohols. The hydrophilic particles are discharged or entrained into the concentrate along with lamellar fluid and do not attach the bubbles by “true flotation”.

On observation during tests, the behavior of the FragC0 and SphC0 at different froth heights (60/80 cm columns) are same during the flotation test, characterized by small-bubble, remaining stable and watery froth. Initially, the foam size little different and the froth is darker, which indicates the entrainment of ultrafine magnetite particles. In Appendix 14, the first overflow appearance of each particle is presented. Then the froth quickly becomes more uniform and whiter at higher froth heights as the experiment proceeds.

An increase in froth height results in a longer froth rise time, allowing more drainage of water and solid particles. The mass and water recovery diagram (found in Appendix 1) shows decrease in entrainment and a reduction in the concentrate's product content with increasing froth height. This observation aligns with the findings of X. Zheng et.al (21), which indicate that the lower froth height results in a wetter froth that contains more liquid and unwanted gangue minerals. Moreover, the FUERSTENAU diagram (in Appendix 4) depicts that glass particles are slightly more entrained than magnetite.

Spheres are more likely to be entrained in the lamellar liquid compared to fragments at different froth heights (60/80/100 cm) in Figure 24. The observation that spherical particles are more likely

to be entrained in lamellar fluid than fragments aligns with Little et al. (23) found that spherical particles have higher entrainment than non-spherical particles, while contradicts with results of Wiese et al. (22). Additionally, the froth height's effect varies, with an increase in froth height leading to a decrease in entrainment degree, as seen in the ENT graph (Appendix 11). The findings are also evident in both the FUERSTENAU diagram (Appendix 4) and the HALBICH diagram (Figure 24).

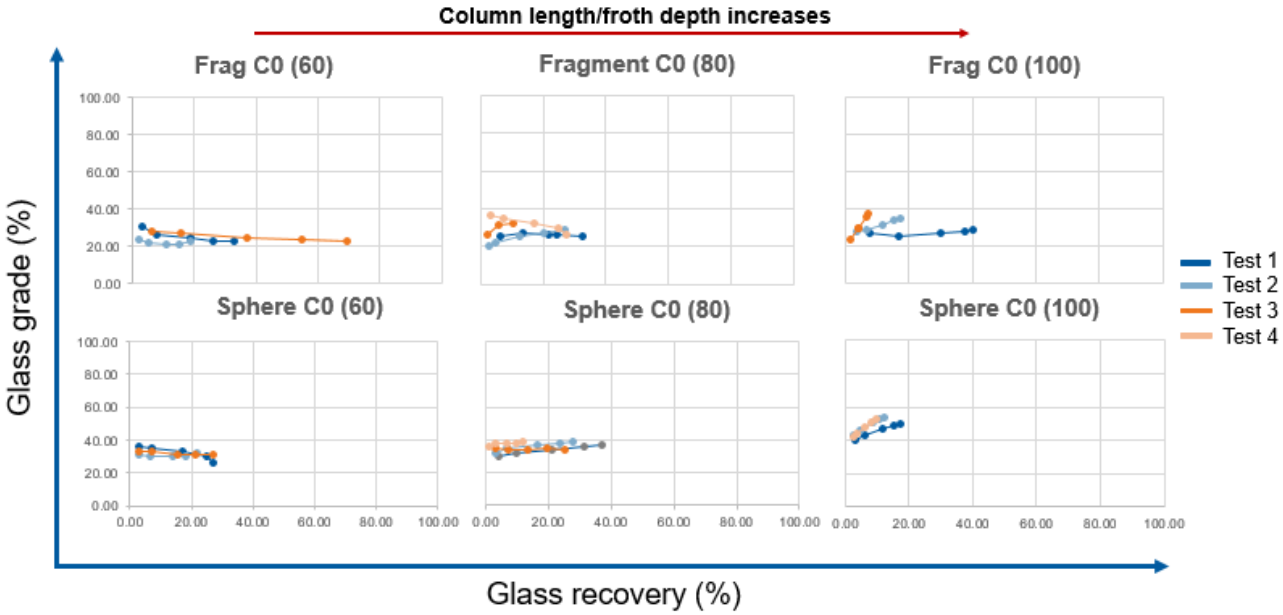

Figure 24 Halbich diagram of flotation tests (Test 1-4) in SphC0 and FragC0 at 60/80/100 cm columns (Rotor speed at 600 rpm and Air rate at 0.9 l/min)

Fragment / Sphere C6:

Medium hydrophobicity particles of SphC6 show higher selectivity compared with FragC6 particles in both HALBICH as shown in Appendix 8 Halbich diagram – Grade and recovery of FragC6 and SphC6 particles at 60/80/10 cm columns (Test 1-4) and FUERSTENAU diagram (see Figure 25). This observation of flotation efficiency based on evaluation diagrams is supported by the selectivity index (SI) table. However, the results contradict with results of Koh et al (25).

The mass and water recovery diagram curve (see Appendix 2) shows that the SphC6 and FragC6 have lower mass and water recovery as froth height increases due to water drainage by gravitational force. When a stable froth structure with a higher mass recovery indicates a greater particle load on the froth.

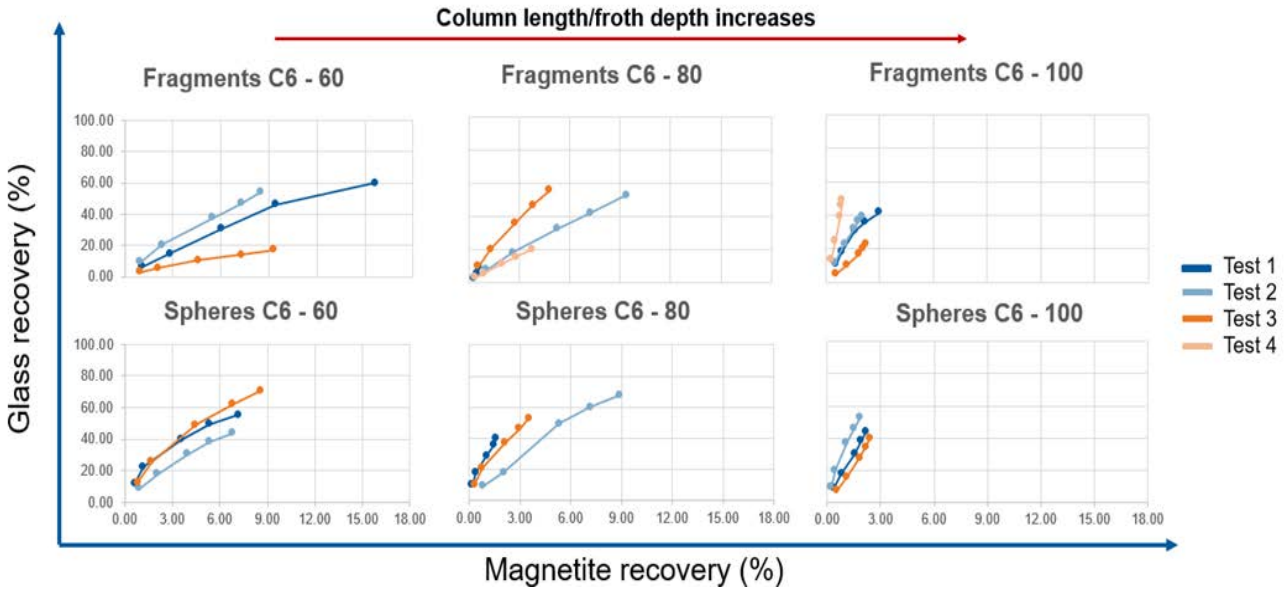

Figure 25 Fuesrstenau upgrading curve of flotation test (Test 1 – 4) in SphC6 and FragC6 at 60/80/100

On observation during the experiment, the froth formation becomes different bubbles-particle aggregation and rather unstable at the first minute. The appearance of froth is darker due to the entrainment of ultrafine magnetite particles into the concentrate. As the experiment progressed, the appearance of froth is stable and whiter. The stability and froth formation of SphC6 and FragC6 become uniform and stable normally after 2 min at 60 cm and 3-4 min at 80 cm columns.

Fragment C10 / Sphere C10:

The appearance of the highly hydrophobic SphC10 and FragC10 are the same and strongly destabilize the froth phase during the flotation experiment due to bubble coalescence and collapsing while the froth layer forms and rises

Figure 26 shows the froth behavior changes over time (5 sec, 25 sec, and 1 min) at 60 cm column for both FragC10 and SphC10. FragC10 and SphC10 are unstable, more watery, and dark froth structures in experiment observation, which indicates the ultrafine unwanted magnetite particles. SphC10 significantly changed the froth phase behavior and the froth becomes stable and uniform in the first minute. While, FragC10 is characterized by unstable and different large-small bubble sizes, and the froth becomes stable and uniform after 2 minutes at a 60 cm column.

A previous study of MultiDimFlot project, Nora Stefenelli (30) observed that SphC10 has large, unstable bubbles in the first 2 min, but after ultrafine magnetite particles is entrained, the bubbles transform into very stable froth loaded with valuable substances. However, four tests were performed in FragC10 but two of them is discontinued due to insufficient overflow after 10 minutes

of rising time. Another two of them resulted in the collection of only one or two concentrates with a high recovery of glass particles (30).

In the HALBICH diagram (see Appendix 9), FragC10 exhibits greater selectivity compared to SphC10, a finding supported by the FUERSTENAU diagram (see Appendix 6) and selectivity Index (SI) value results (see Appendix 10). The effect of particle shape on the flotation process indicates that non-spherical particles show higher wettability and destabilizing effect than spherical particles as a research findings (24) (25). Furthermore, the high degree of hydrophobicity particles can also destabilizing effect on the flotation process (24). Fragments have a higher hydrophobicity state than spherical particles as presented by Sygusch & Rudolph (4). Consequently, FragC10 possesses the most significant destabilizing effect, whereas SphC10 does not. Flotation tests for FragC10 at 60 and 80-cm column heights were successful in low froth heights. However, at 100 cm column height, deep froth and combined destabilizing and highly hydrophobic properties impeded the process.

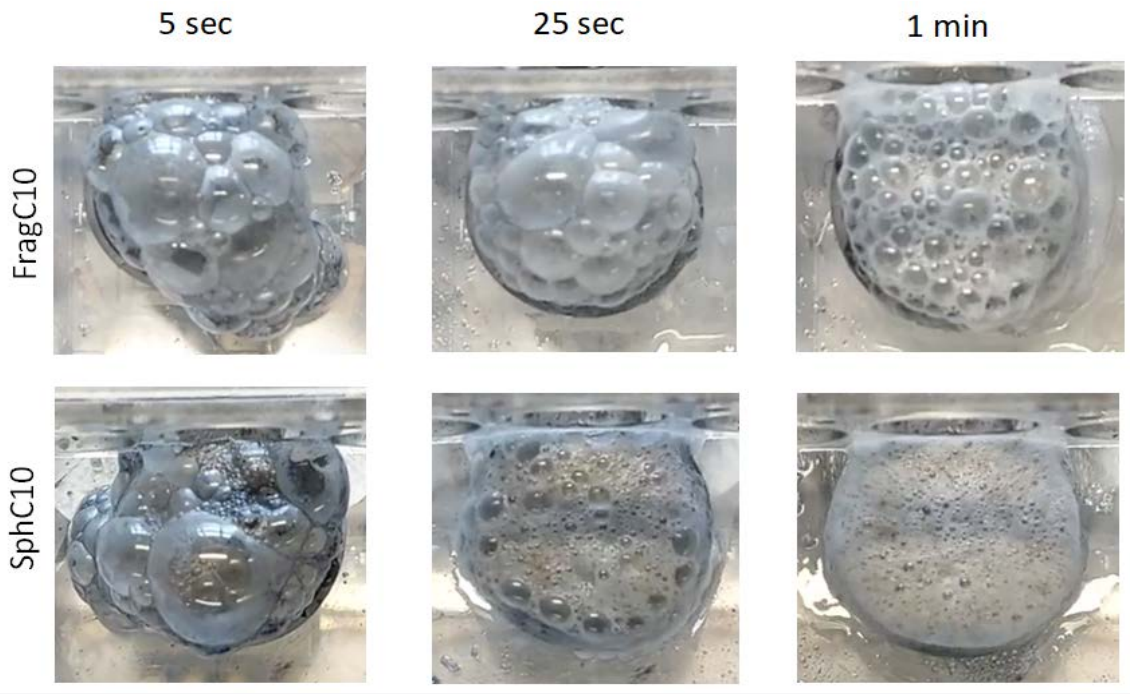

Figure 26 Change in froth behavior during flotation test: FragC10 (top) and Sph10 (bottom) in 5 sec, 25 sec and 1 min after first overflow at 60 cm column

The mass and water recovery diagram (see Appendix 3) depicts that SphC10 particles have a higher particle load on the froth compared to FragC10 at 60 & 80 cm columns due to longer rise time and destabilizing effect on the flotation process. However, it is impossible to compare

SphC10 and FragC10 at 100 cm column due to the experiment discontinuation of FragC10 as I mentioned above.

4.2 Influence of hydrophobicity state with constant grain shape at different froth height

60 cm column: According to the HALBICH diagram, increases hydrophobicity state leads to rise selectivity of glass particle for each particle system, which is further supported by FUERSTENAU diagram. Mass and water recovery diagram (see Appendix 15) shows that varying hydrophobicity state and shaped particles have nearly the same mass and water recovery outcomes at 60 cm due to lower froth height.

80 cm columns: Mass and water recovery diagram (see Appendix 16) illustrates that as hydrophobicity increases, water recovery decreases for Fragments, but there is no significant difference observed for Spheres. HALBICH diagram (see Appendix 22) indicates that the increasing froth height with the higher selectivity. SphC0 and FragC0 are similar appearances in the HALBICH diagram. The selectivity of SphC6 is found to be higher than FragC6, as supported by the FUERSTENAU diagram (see Appendix 19) and selectivity index (SI) (Appendix 10).

Conversely, FragC10 demonstrates greater selectivity compared to SphC10 in both HALBICH (Appendix 22) and FUERSTENAU diagram (see Appendix 19). The degree of hydrophobicity and particle shape is primary factors affecting froth stability. FragC10 influences a greater destabilizing effect on froth due to its higher hydrophobicity state and rough surface characteristics. In the flotation test at 80 cm column, the froth rise time (Appendix 12) in FragC10 is longer due to high froth height and highly destabilizing effect. Increased froth height leads to a longer froth rise and residence time, as result in then drainage of lamellar liquid and solids, which in turn results in higher selectivity of glass particles.

100 cm column: The mass and water recovery diagram (see Appendix 17) indicates that particles with medium hydrophobicity exhibit high water and mass recovery, and as hydrophobicity increases, water recovery decreases accordingly. Johansson and Pugh (24) found that medium hydrophobicity particles become attached to the air/solution interface, which enhances the rigidity of the froth structure and creates stable froth. When a stable froth structure with a higher mass recovery indicates a greater particle load on the froth. Hydrophilic particles have lower mass and water recovery due to the higher froth height, which is related to increased drainage of lamellar liquid.

The HALBICH diagram (see Appendix 23) reveals that glass particles (SphC6) have greater selectivity than FragC6 at a 100 cm column, a finding supported by the selectivity index value (SI) and FUERSTENAU diagram (see Appendix 20). SphereC10 has the lowest water recovery and the most effective separation among the particle systems.

4.3 Error observation

The Flotation test involves numerous processes, measurements, and calculations, and is influenced by many errors. In this chapter, we discussed the error factors on the flotation process.

- Weighing procedure is conducted during the preparation, main flotation test, and post-processing of a flotation process. Analytical balance accuracy is ±0.01 g in the laboratory. The number of weighing steps during the flotation test contribute significantly to the total error.
- All main flotation tests were performed by the same person. However, the preparation and post-processing procedure is accomplished by cooperation work with substituting the person. These will generate random errors due to human influence.
- Due to long-term storage in a bottle, some glass particles occasionally agglomerated and become unbreakable. Although rare, the presence of such particles in the feed suspension may have influenced on experimental outcomes.
- The MultiDimFlot separation apparatus itself is the primary source of error affecting both the flotation process and the resulting concentrate. As a newly designed separation apparatus, it consists of numerous individual components, making it more complex than conventional flotation cells. Issues with improper assembly and wear can lead to seal failure as a result of slurry loss by leaking between inadequately connected parts.

5 Conclusion and Outlook

The objective of this study is to investigate the influence of the froth height on separation outcome and how the fractionating behavior within the froth is affected by the different particle properties (wettability state, morphology). The feed suspension consisted of a constant liquid phase and a binary mixture of magnetite as a non-floatable fraction and differently shaped glass particles as a floatable fraction in a consistent mass ratio. The gangue mineral magnetite retained its original grain shape and size. The glass particles has various shapes (spheres and fragments) and each glass particle morphology is available in three different wettability states, i.e. hydrophilic (C0), medium hydrophobic (C6), and strongly hydrophobic (C10). Consequently, six different glass particle fractions with defined particle properties are available for flotation, and their separation success was assessed through established visualizations such as the HALBICH diagram, FUERSTENAU diagram and characteristic values like the selectivity index SI, and the degree of entrainment (ENT).

The experimental work addresses various aspects of the topics, investigating the effects of ultrafine particle properties (wettability state and particle shape) on different froth heights, as well as the influence of froth height on different particle systems. The main findings can be summarized as follows in below:

1. Flotation results of hydrophilic particles align with research results of Little et al (23) that sphere particles exhibit a higher tendency to be entrained in lamellar fluid compared to fragments at various froth heights (60/80/100). An increase in froth height results in a longer froth rise time, leading to greater drainage of water and solid particles, resulting in a low amount of product.
2. Medium hydrophobic particles reach high froth stability and yield a large quantity of product. SphC6 exhibits higher selectivity compared with FragC6 particles at different froth heights (60/80/100). Our findings contradict the particle shape factors that rough surface particles have higher attachment efficiency compared to spherical particles. As froth height increases, selectivity improves while the quantity of concentrated product decreases.
3. The froth stability is primarily influenced by the degree of hydrophobicity and particle shape. FragC10 demonstrates higher selectivity and rougher surface, both contributing to a significant destabilizing impact on flotation. In the flotation test at 80 cm, the longer froth rise time is attributed to higher froth height and the destabilizing impact, leading to enhance drainage of lamellar liquid and solid particles. This results in a greater selectivity of glass particles compared to SphC10. However, at a column height of 100 cm, deep froth and

combined destabilizing influence, along with highly hydrophobic properties obstructed the flotation process. Consequently, the flotation efficiency cannot be solely determined by a single parameter, as other factors can interact and influence the separation process.

4. Referring to Figure 9 on the left side, it can be seen that the ENT approaches 1 for ultrafine particles. This observation highlights the effectiveness of the deep froth in MultiDimFlot, as evidenced by the reduction in ENT values (found in Appendix 11) with increasing in froth height. These findings align with the influence of froth height on the degree of entrainment (ENT) measure as postulated by Zheng et al (21).
5. The findings of the study indicate that particle shape exhibits different characteristics during the flotation process at various hydrophobicity states, but it is seen that the non-spherical particles have a greater destabilizing effect in highly hydrophobic state. Increased hydrophobicity results in higher selectivity and improve destabilizing effect. The shape factors and surface wettability are evaluated together.
6. The result of an increase froth height leads to a longer froth rise time as well as the drainage of lamellar liquid and solids, which result in higher selectivity of valuable minerals and low amount of product.

Froth height and particle characteristics (shape and wettability state) influence froth stability and flotation process efficiency in various ways. Separation success diagrams (FUERSTENAU and HALBICH), selectivity index (SI), and ENT values offer insights into the effectiveness of the flotation process. However, it is difficult to make a concise and accurate conclusion due to the complexity of the factors involved.

For future research in MultiDimFlot, it is suggested to increase the number of repetitions for each experiment. In this study, all flotation tests were conducted at least three times per particle system at various froth heights. While the collected data may provide sufficient for analysis, however, increasing the number of repetitions would contribute to more-in depth studies, leading to more robust analyses and accurate results. It is recommended to perform the experiments at least five times for more reliable outcomes. Future research on MultiDimFlot should investigate its performance in processing natural complex ores, as this would provide valuable insights into its practical applications.

Reference

1. W. J. Trahar LJW. The Flotability of very fine particles - A review. International Journal of Mineral Processing. 1975 December; 3: 103-131.

2. Tommi Huhtamäki XTJTKRHAR. Surface-wetting characterization using. Nature Protocols. 2018 July; 13: 1521-1539.

3. Maurice C. Fuerstenau GJJRHY. Froth Flotaiton: A Century of Innovation Colorado: SME; 2007.

4. Johanna Sygusch MR. A contribution to wettability and wetting characterisation of ultrafine particles with varying shape and degree of hydrophobization. Applied Surce Science. 2021 November; 566.

5. Greg Harbort DC. Fluctuations in the popularity and usage of flotation columns – An overview. Minerals Engineering. 2017 January; 100: 17-30.

6. Barry A. Wills JF. Wills' Mineral Processing Technology. In.: Elsevier; 2015. p. 265-380.

7. N. Ahmed GJJ. The effect of bubble size on the rate of flotation of fine particles. International Journal of Mineral Processing. 1985 April; 14(3): 195-215.

8. Yianatos J. Column Flotation Modelling and Technology. Valparaso: University of Santa Maria, Chemical Engineering Department ; 1989.

9. Hoang HD. Flotation beneficiation of apatite in carbonate-rich and finely disseminated sedimentary phosphate ores in Vietnam. Thesis. Freiberg: Technische Universität Bergakademie Freiberg, Mechanical, Process and Energy Engineering; 2019.

10. Sterbik N. Design of experiments for laboratory batch flotation. Freiberg: HHelmholtz-Zentrum Dresden-Rossendorf, Helmholtz Instite in Freiberg; 2016.

11. Schubert H. On the optimization of hydrodynamics in fine particle flotation. Minerals Engineering. 2008 November; 21(12-14): 930-936.

12. Jovica Sokolovic SM. The effect of particle size on coal flotation kinetics: A review. Physicochemical Problems of Mineral Processing. 2018 July; 54(4): 1172-1190.

13. Jinyoung Je DLJKHC. Simulation of bubble–particle attachment process and estimation of attachment probability using a coupled smoothed particle hydrodynamics–discrete element method model. Minerals Engineering. 2022 June; 183: 107581.

14. Tatu Miettinen JRDF. The limits of fine particle flotation. Minerals Engineering. 2010 April; 23(5): 420-437.

15. Ahmadi Rahman KDAAMFM. Nano-microbubble flotation of fine and ultrafine chalcopyrite particles. Mining Science and Technology. 2014 July; 24(4): 559-566.

16. Behzad Vaziri Hassas HCOGFKMCMSC. Effect of roughness and shape factor on flotation characteristics of glass beads. Colloids and Surfaces A: Physicochemical and Engineering Aspects. 2016 March; 492(5): 88-99.

17. David I. Verrelli WJBPTLKMPSBF. Particle shape effects in flotation. Part 1: Microscale experimental observations. Minerals Engineering. 2014 April; 58: 80-89.

18. Singh N. Factors driving entrainment in flotation systems and. Thesis. Montreal: McGill University, Mining and Materials Engineering; 2013.

19. Chao Wang CSQL. Entrainment of Gangue Minerals in Froth Flotation: Mechanisms, Models, Controlling Factors, and Abatement Techniques—a Review. Mining, Metallurgy & Exploration. 2020 August; 38: 673-690.

20. Wang L. Entrainment of Fine Particles in Froth Flotation. Thesis. The University of Queensland, Sustainable Minerals Institute; 2016.

21. X. Zheng NWJJPF. Modelling of entrainment in industrial flotation cells: Water recovery and degree of entrainment. Minerals Engineering. 2006 August; 19(11): 1191-1203.

22. J.G. Wiese CTO. An investigation into the relative role of particle size, particle shape and. International Journal of Mineral Processing. 2016 June; 156: 127-133.

23. Lucy Little JWMBAMVR. Investigating the effects of particle shape on chromite entrainment at a platinum concentrator. Minerals Engineering. 2016 October; 96-97: 46-52.

24. G. Johansson RJP. The influence of particle size and hydrophobicity on the stability of mineralized froths. International Journal of Mineral Processing. 1992 January; 34(1-2): 1-21.

25. P.T.L. Koh FPHLKSTTCWJB. The effect of particle shape and hydrophobicity in flotation. International Journal of Mineral Processing. 2009 October; 93(2): 128-134.

26. Achaye I. Effect of particle properties on froth stability. Thesis. Cape Town: University of Cape Town, Department of Chemical Engineering; 2017.

27. Johanna Sygusch MR. The effect of the particle parameters of morphology and wettability in ultrafine particle flotation and froth fractionation. IMPC 2020: XXX International Mineral Processing Congress. 2020 October.

28. Sigma-Aldrich. [Online]. Available from: https://www.sigmaaldrich.com/MN/en/technical-documents/technical-article/materials-science-and-engineering/drug-delivery/polyethylene-glycol-selection-guide.

29. Sigma-Aldrich. [Online].; 2022 [cited 2022 April 04. Available from: https://www.sigmaaldrich.com/MN/en/sds/sial/p4338.

30. Stefenelli N. Investigation into the flotation of ultrafine particles in the newly designed MultiDimFlot separation apparatus. Thesis. Freiberg: TU Bergakademie Freiberg, Mechanical, process and energy engineering; 2022.

31. BRUKER. BRUKER. [Online]. Available from: https://www.bruker.com/en/products-and-solutions/elemental-analyzers/handheld-xrf-spectrometers/S1-TITAN.html?source=google&medium=cpc&campaign=GSN_|_Asia_-_Tier-2&content=02_-_GSN_|_Products_|_HMP_|_S1_TITAN&s_kwcid=AL!14677!3!634983901663!p!g!s1%20tit.

32. Society AC. American Chemical Society (ACS). [Online]. Available from: https://www.acs.org/molecule-of-the-week/archive.html?archive=All.

33. Ming Li YXCZQLZYRZYZ,YXXG. Effect of roughness on wettability and floatability: Based on wetting film drainage between bubbles and solid surfaces. International Journal of Mining Science and Technology. 2022 November; 32(6): 1389-1396.

34. Michael Haschke JFMH. X-Ray Fluorescence Spectroscopy for Laboratory Applications: Wiley-VCH; 2021.

35. Dunne RC. SME Mineral Processing and Extractive Metallurgy Handbook S. K. Kawatra CY, editor.: ASM International; 2019.

36. Jovica Sokolovic SM. The effect of particle size on coal flotation kinetics: A review. Physicochemical Problems of Mineral Processing. 2018 July; 54(4): 1172-1190.

37. Nummi E. thermofisher. [Online]. [cited 2015 April 7. Available from: https://www.thermofisher.com/blog/mining/technology-focus-x-ray-fluorescence-xrf-in-mining/.

Appendix

Comparison same particle system at different column heights

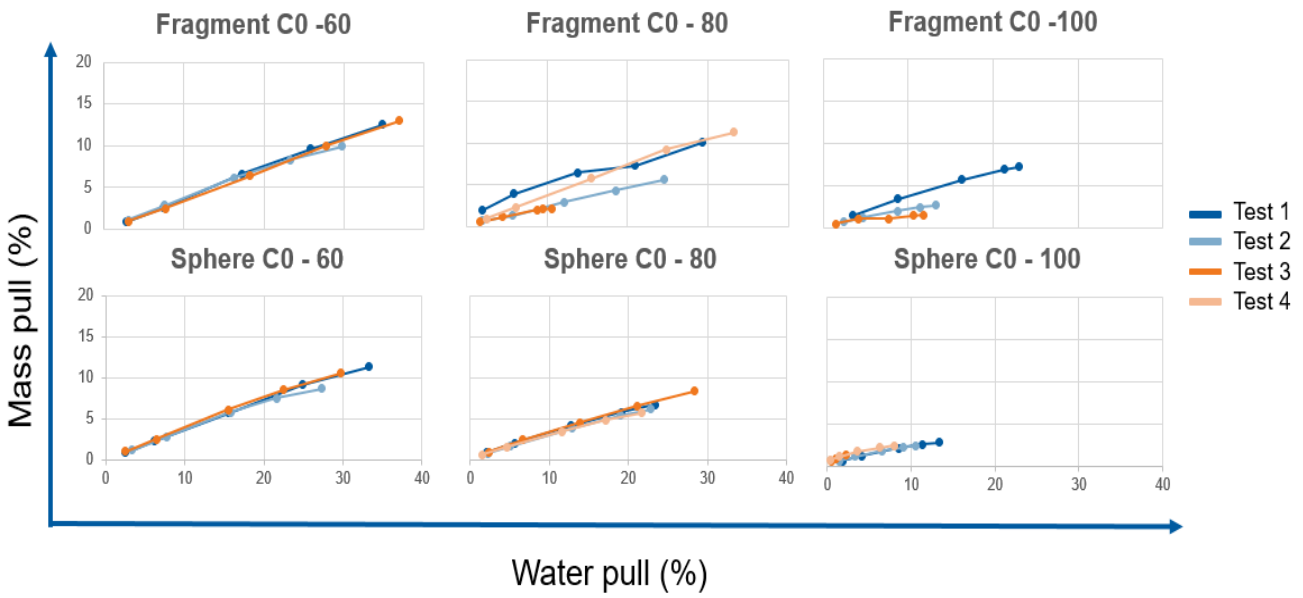

Appendix 1 Mass VS Water pull diagram – FragC0 and SphC0 (Test 1-4) at 60/80/100 cm columns

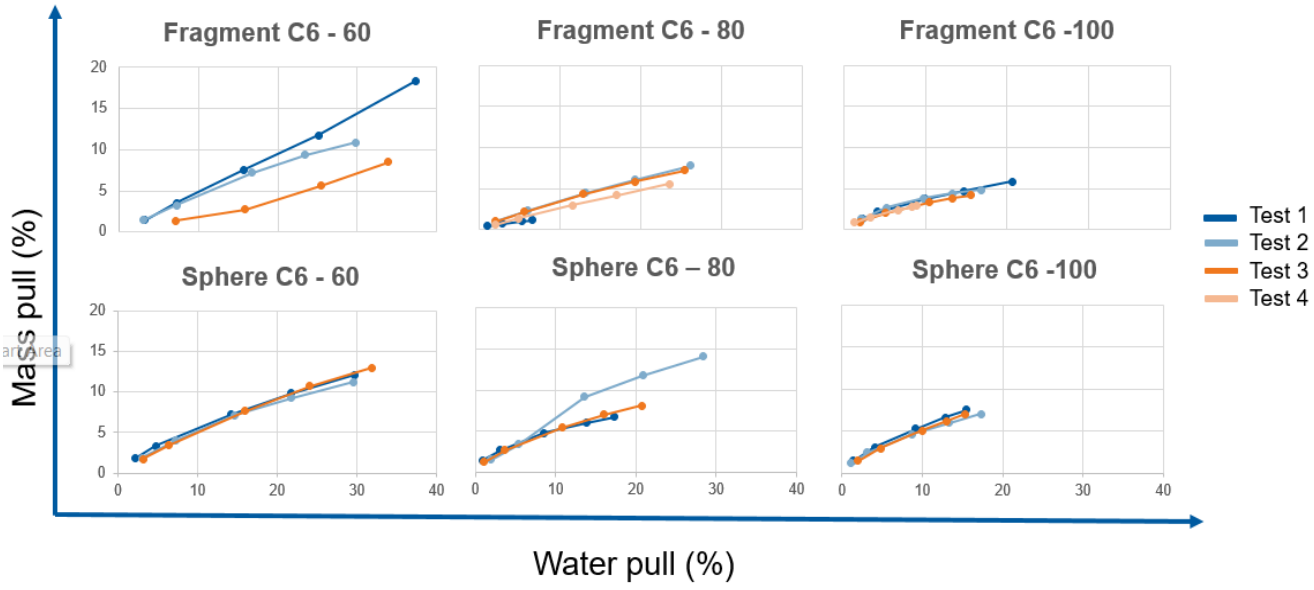

Appendix 2 Mass VS Water pull diagram – FragC6 and SphC6 (Test 1-4) at 60/80/100 cm columns

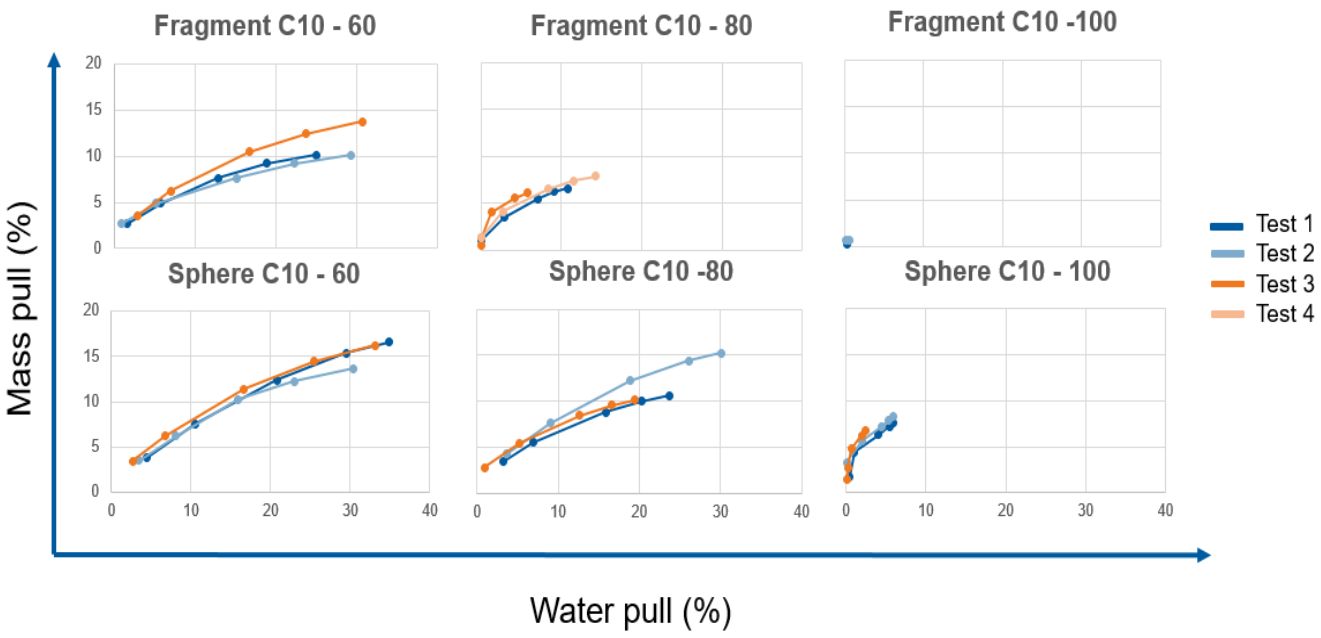

Appendix 3 Mass VS Water pull diagram – FragC10 and SphC10 (Test 1-4) at 60/80/100 cm columns

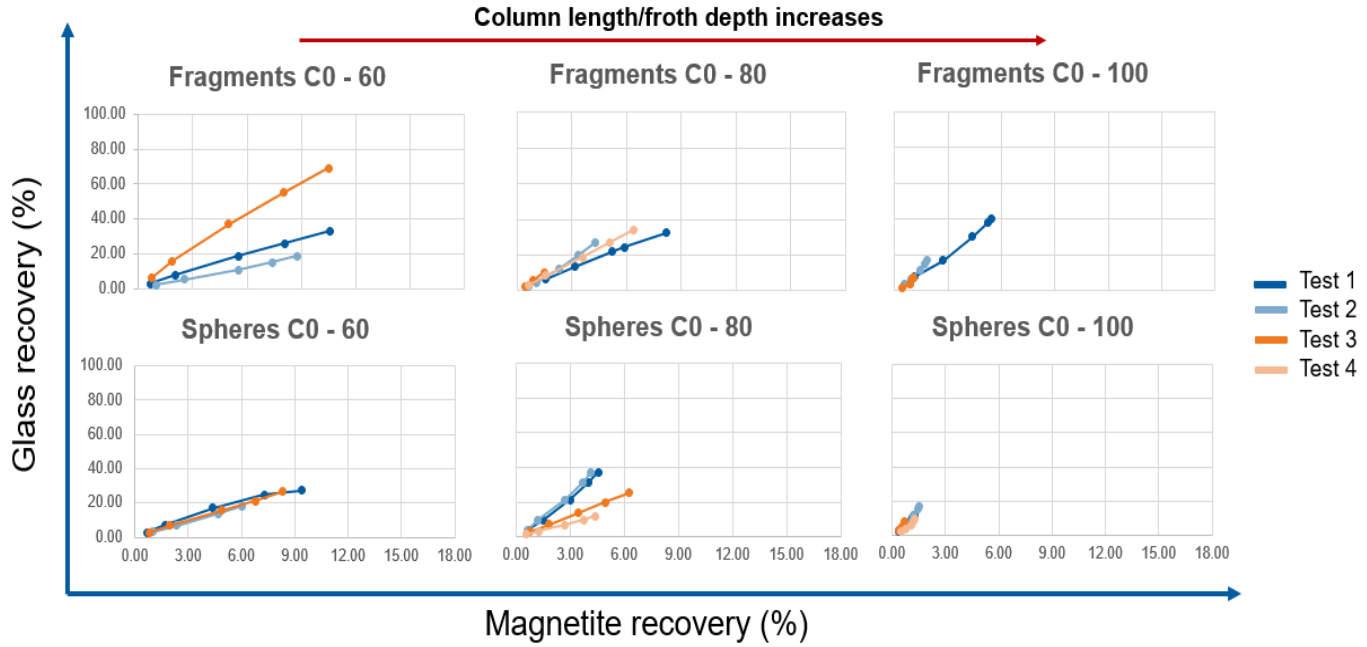

Appendix 4 Fuesrstenau upgrading curve of flotation test (Test 1 – 4) in SphC0 and FragC0 at 60/80/100 cm columns

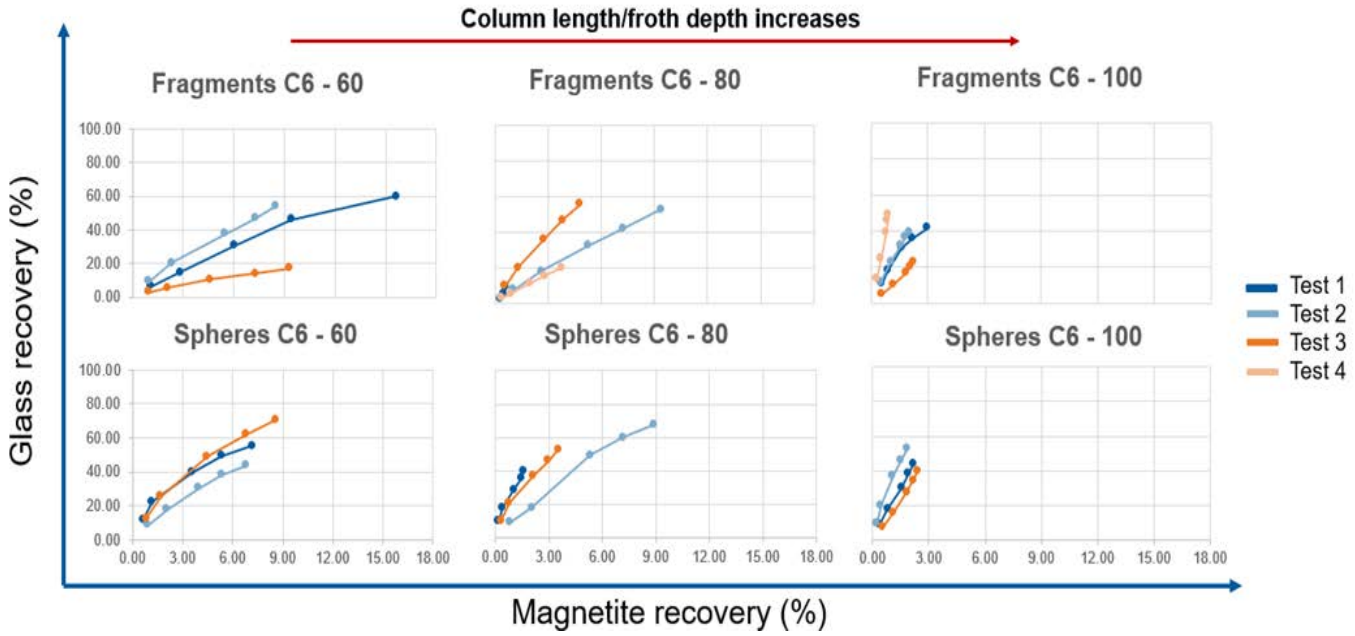

Appendix 5 Fuesrstenau upgrading curve of flotation test (Test 1 – 4) in SphC6 and FragC6 at 60/80/100 cm columns

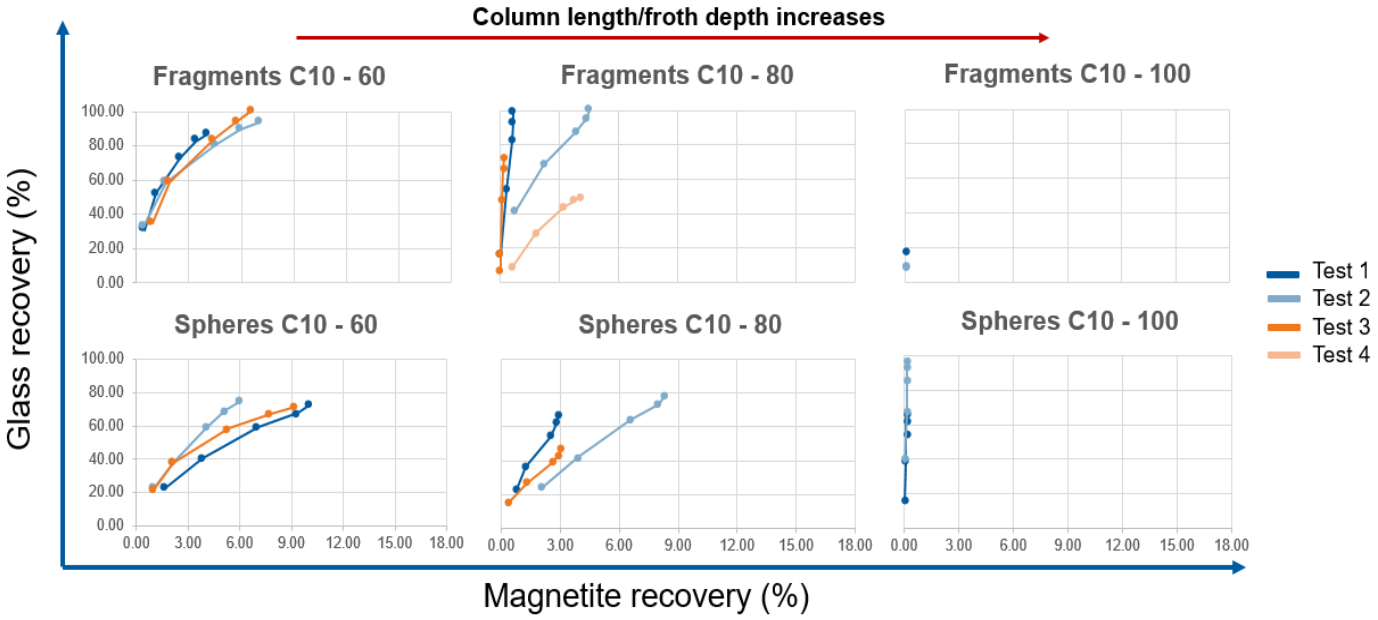

Appendix 6 Fuesrstenau upgrading curve of flotation test (Test 1 – 4) in SphC10 and FragC10 at 60/80/100 cm columns

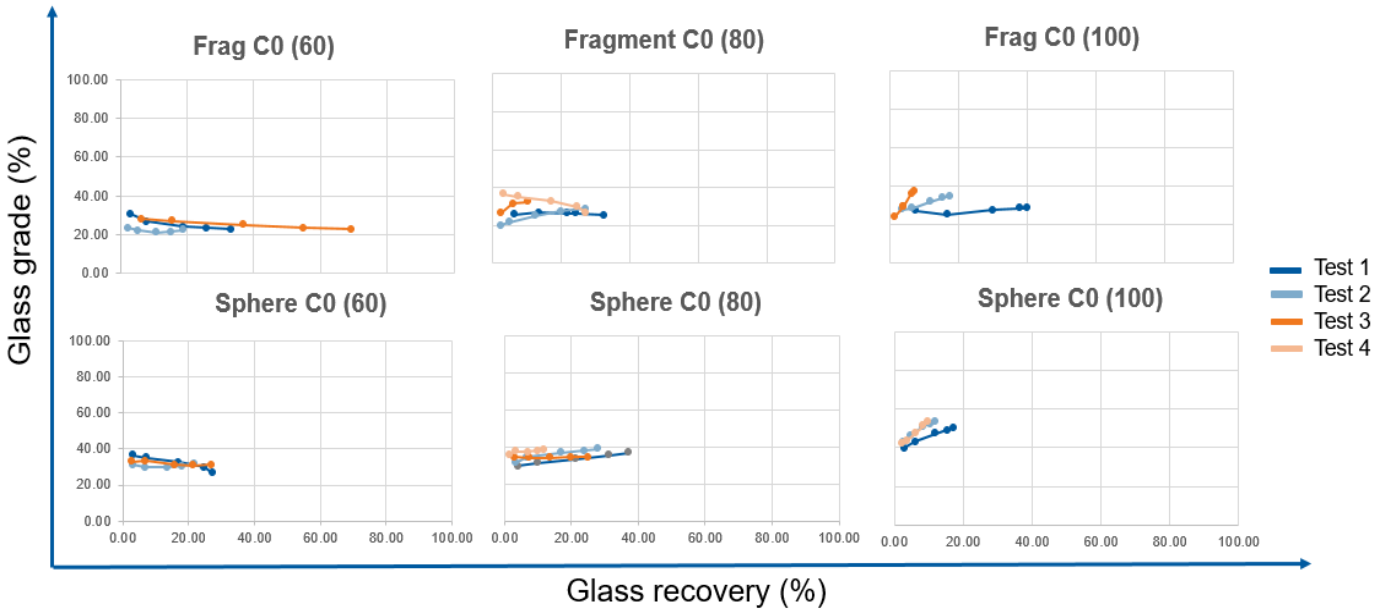

Appendix 7 Halbich diagram – Grade and recovery of FragC0 and SphC0 particles at 60/80/10 cm columns (Test 1-4)

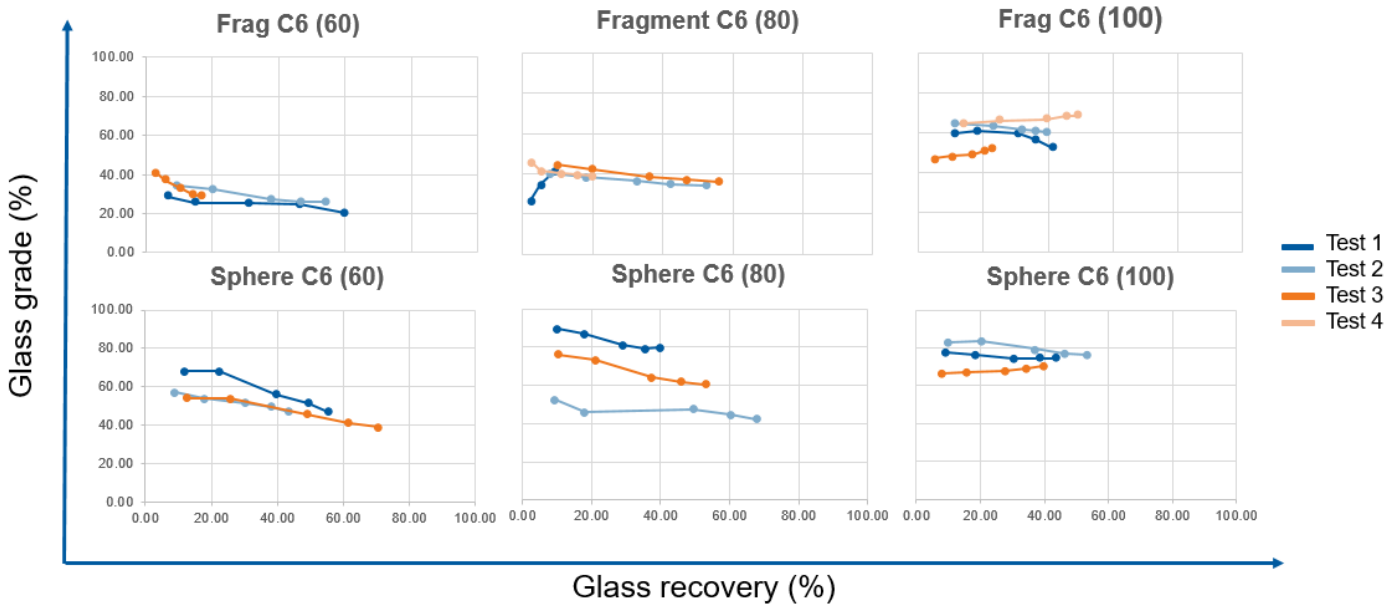

Appendix 8 Halbich diagram – Grade and recovery of FragC6 and SphC6 particles at 60/80/10 cm columns (Test 1-4)

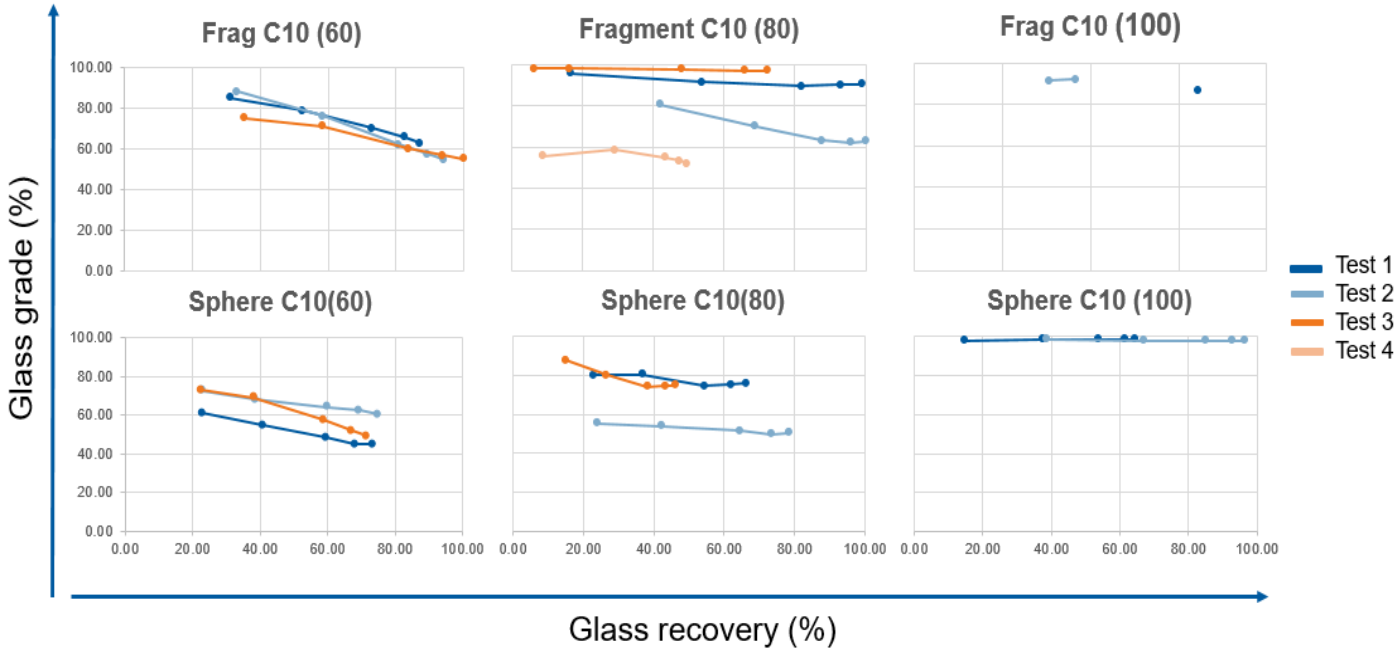

Appendix 9 Halbich diagram – Grade and recovery of FragC10 and SphC10 particles at 60/80/10 cm columns (Test 1-4)

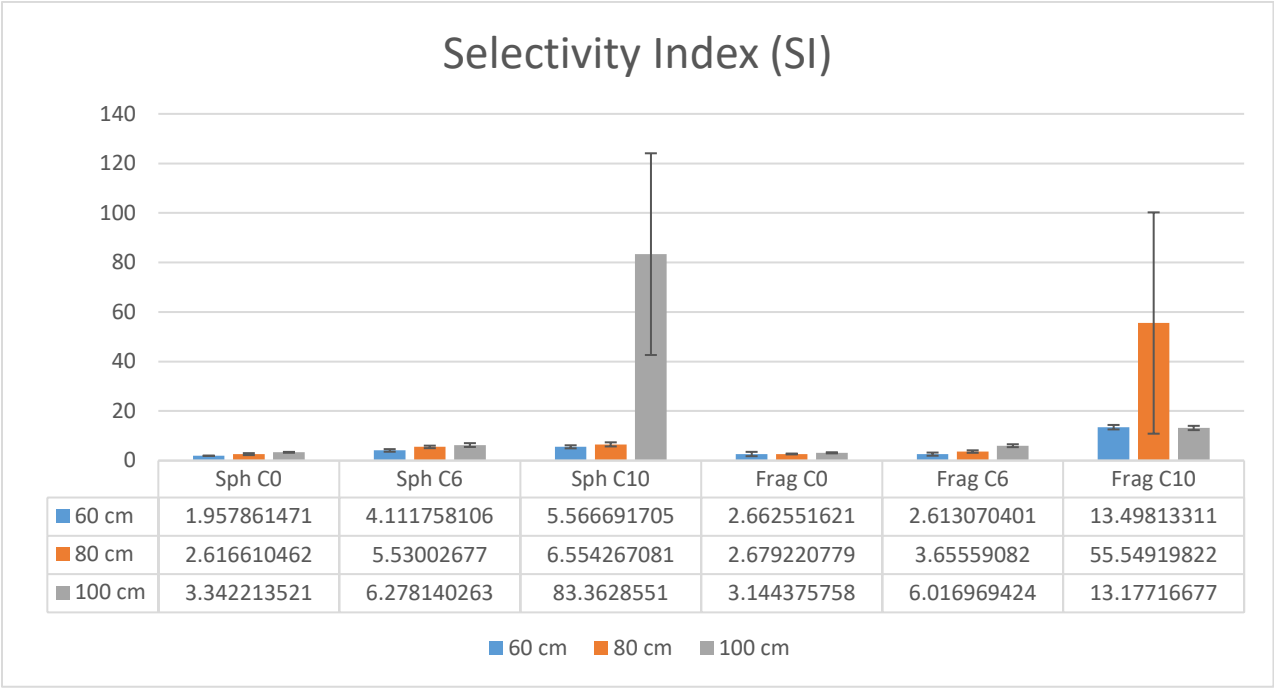

	Sph C0	Sph C6	Sph C10	Frag C0	Frag C6	Frag C10
60 cm	1.957861471	4.111758106	5.566691705	2.662551621	2.613070401	13.49813311
80 cm	2.616610462	5.53002677	6.554267081	2.679220779	3.65559082	55.54919822
100 cm	3.342213521	6.278140263	83.3628551	3.144375758	6.016969424	13.17716677

Appendix 10 Mean value of selectivity index (SI) with error bars.

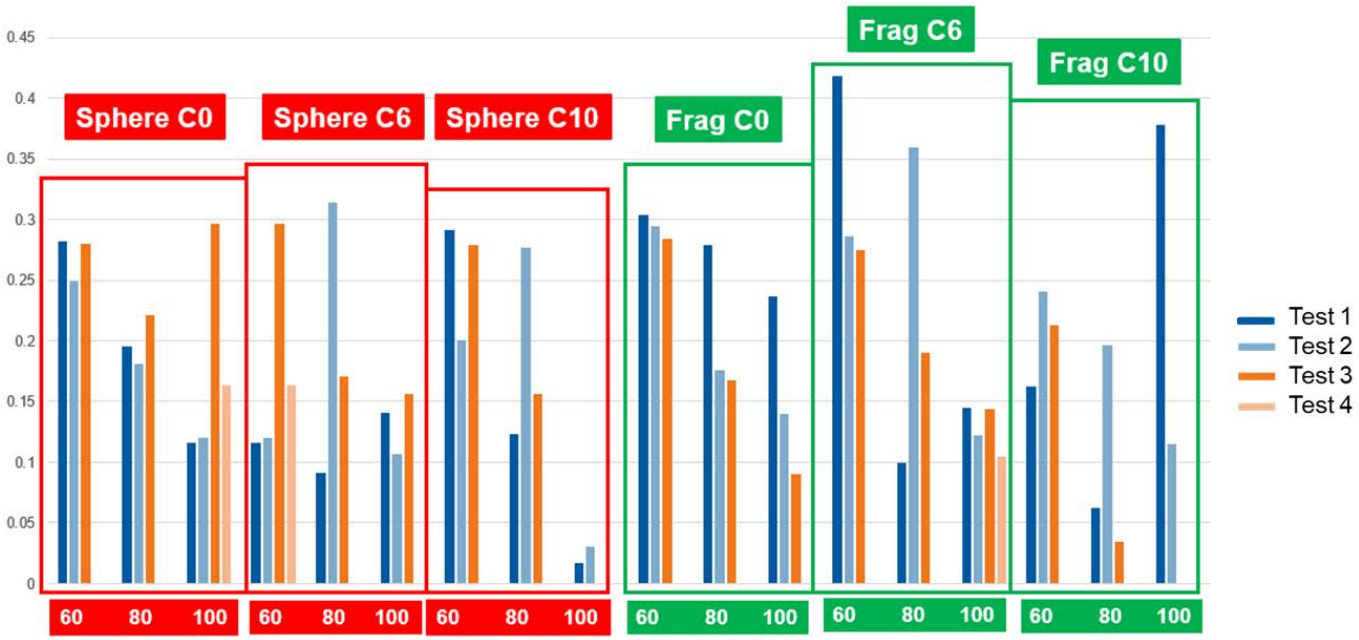

Appendix 11 Entrainment factor (ENT) values at fixed operating parameters (rotor speed at 600 rpm and air rate at 0.9 l/min) in different height (60/80/100 cm columns) – six different parameters.

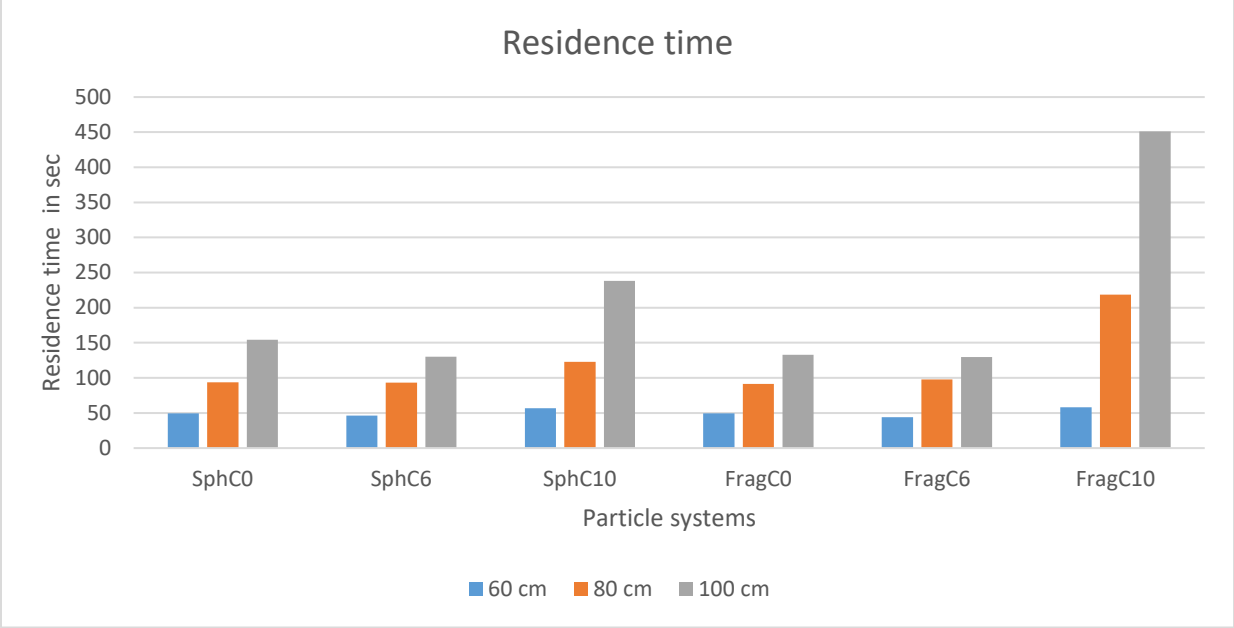

Appendix 12 Recorded froth rise time in different particle systems at different column height (60/80/100)

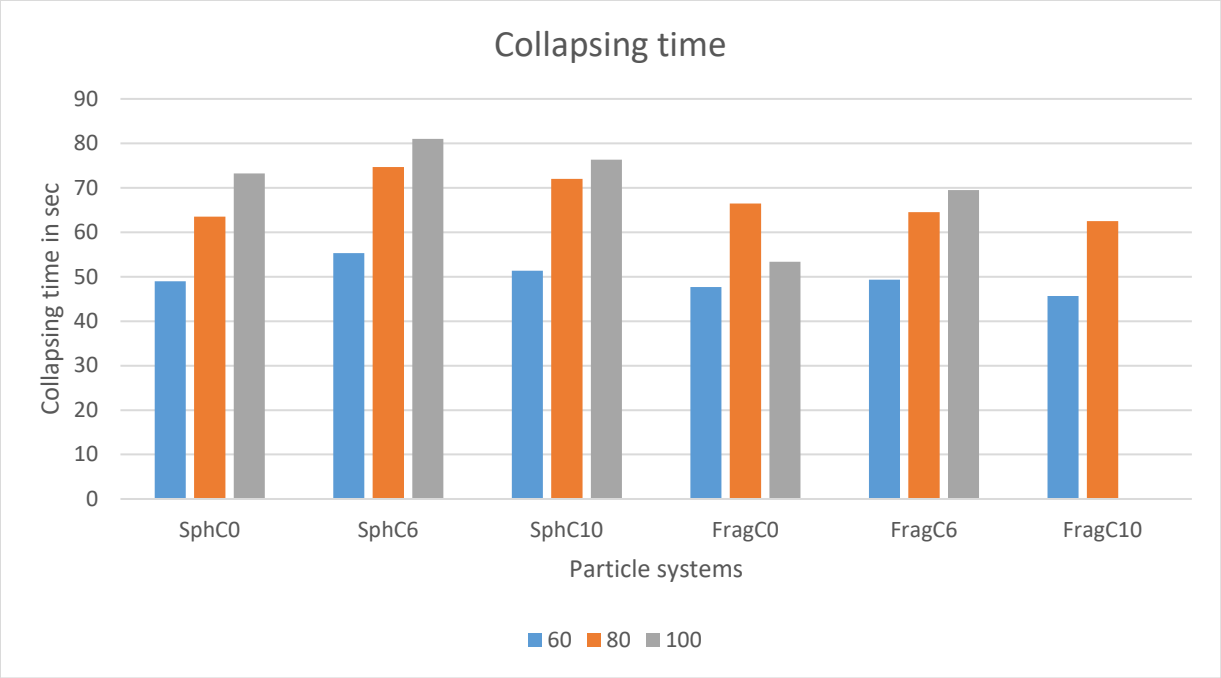

Appendix 13 Recorded collapsing time in different particle systems at different column height (60/80/100)

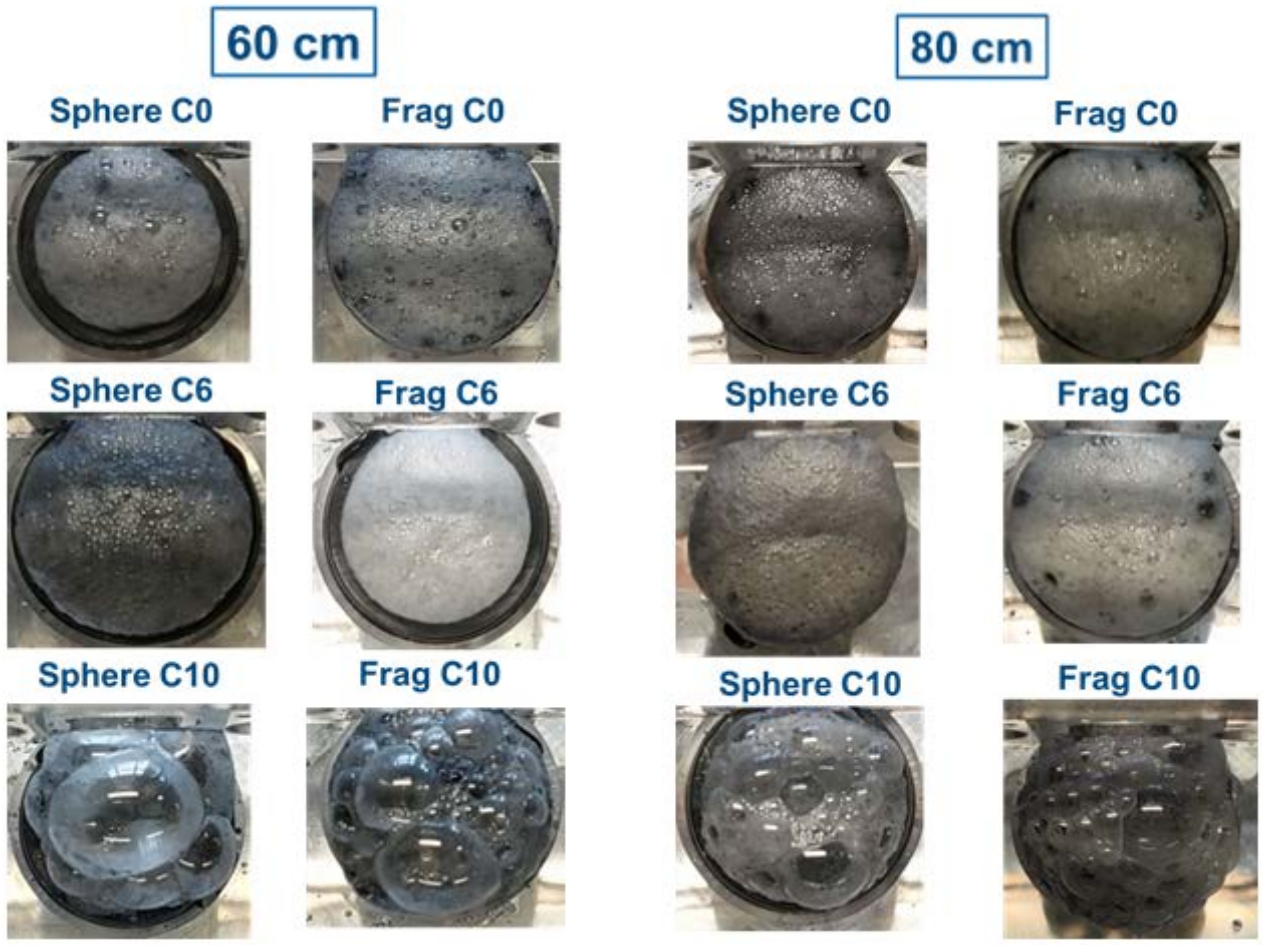

Appendix 14 Appearance of Fragments and Spheres different hydrophobicity state at different froth height (60 & 80 cm column)

Comparison of different particle systems at same column height

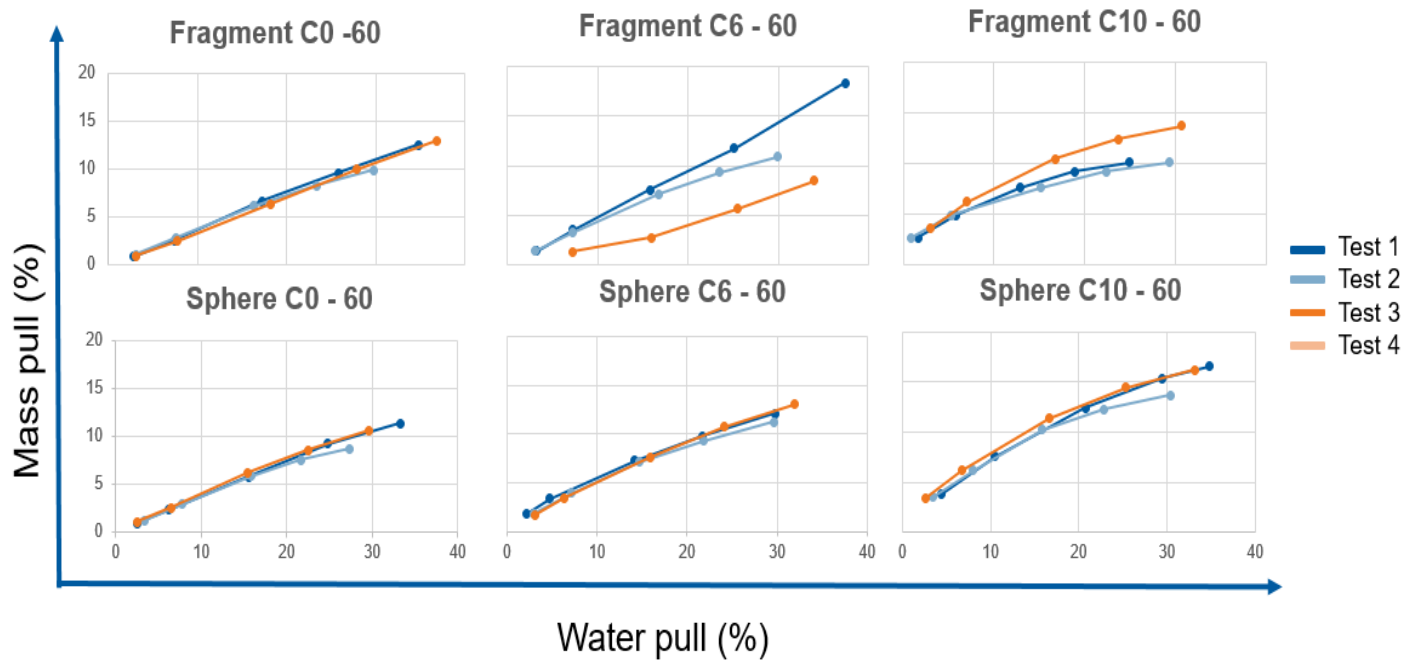

Appendix 15Mass VS Water pull diagram Fragment and Spheres at 60cm column

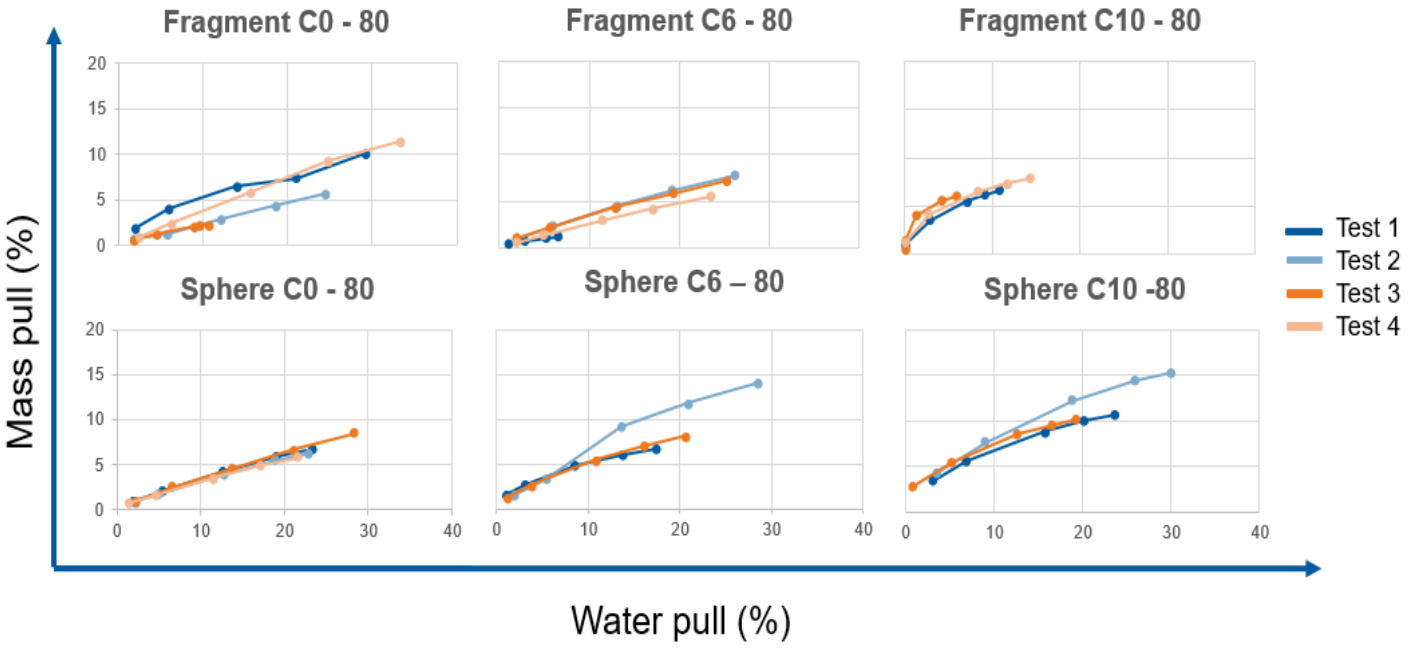

Appendix 16 Mass VS Water pull diagram Fragment and Spheres at 80cm column

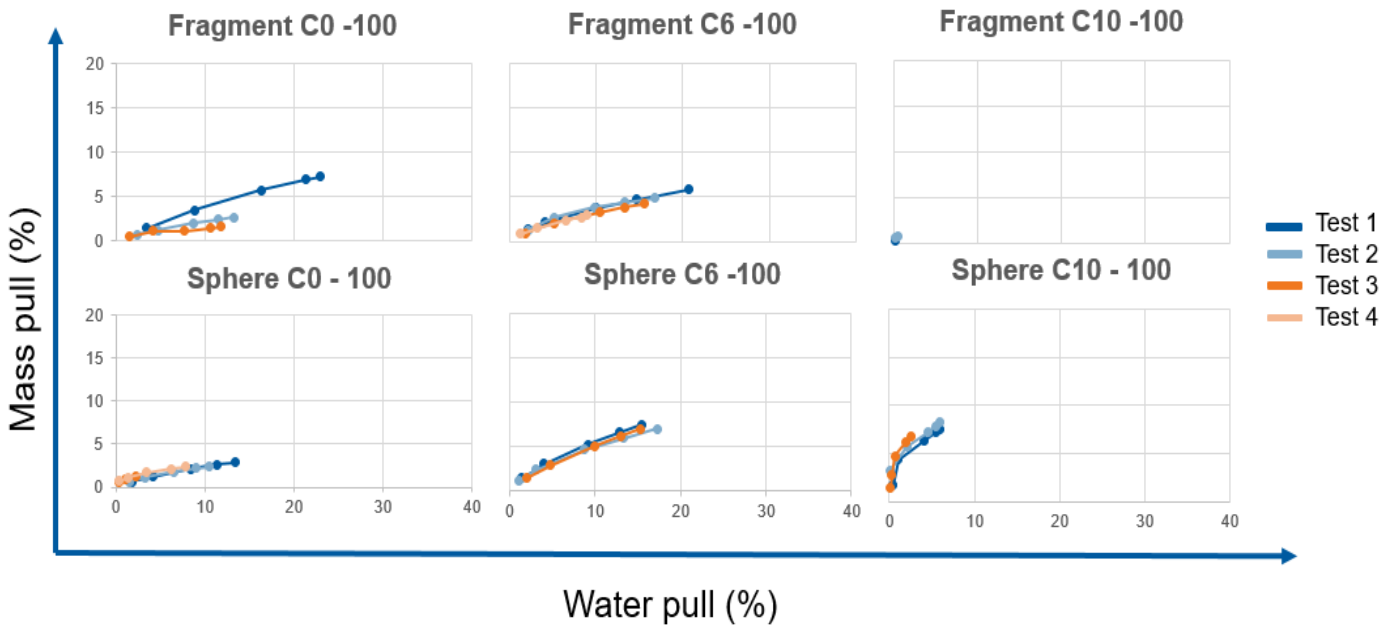

Appendix 17 Mass VS Water pull diagram Fragment and Spheres at 100cm column

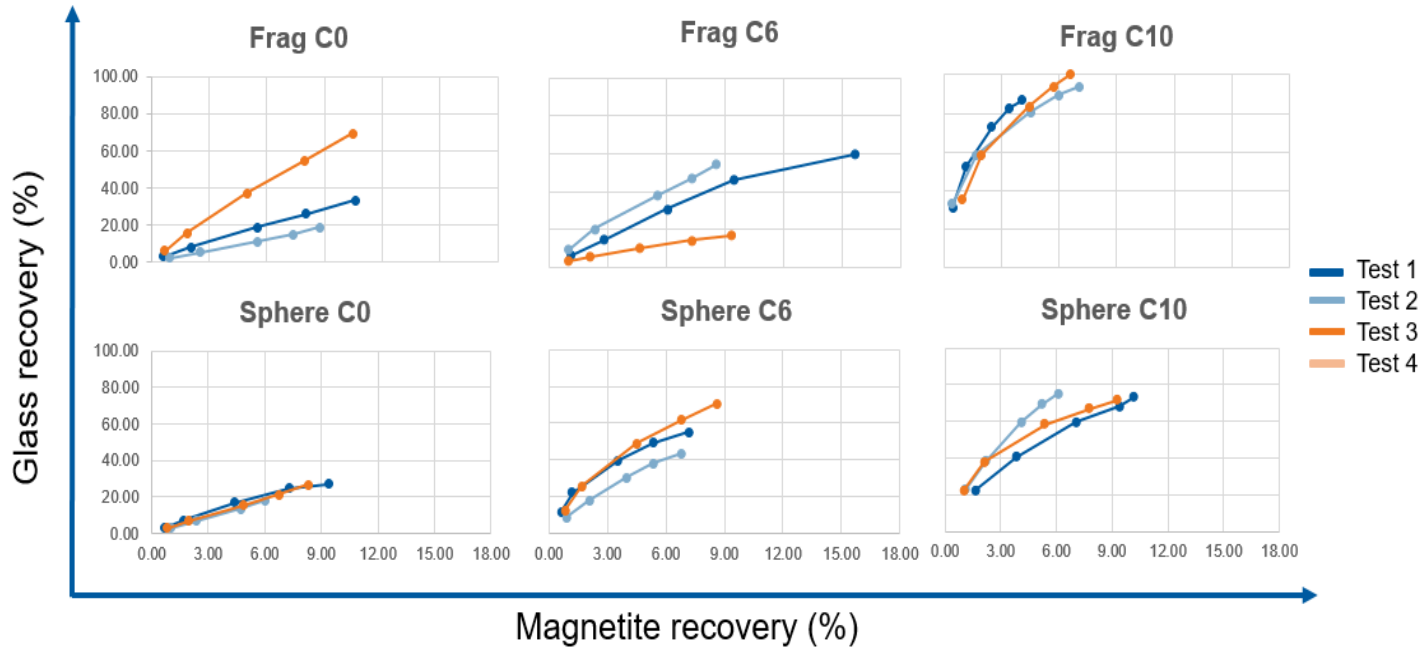

Appendix 18 Fuesrstenau upgrading curve of flotation test at 60 cm column

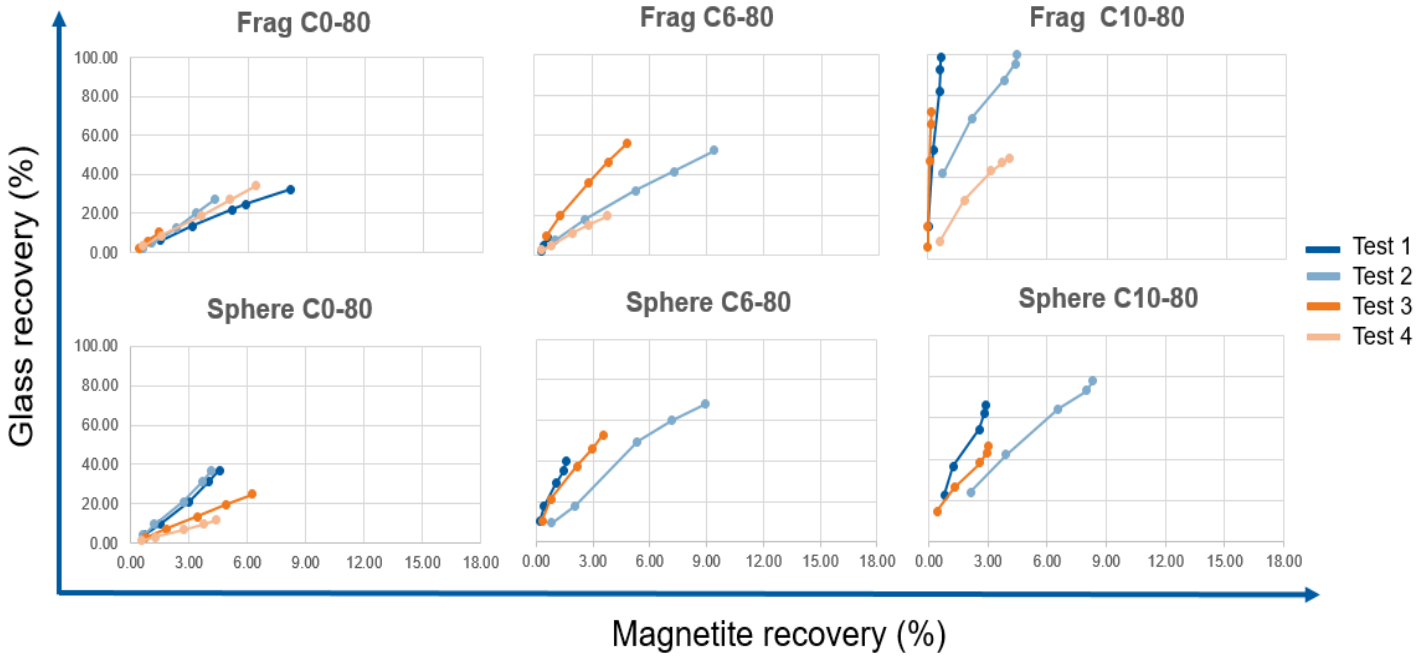

Appendix 19 Fuesrstenau upgrading curve of flotation test at 80 cm column

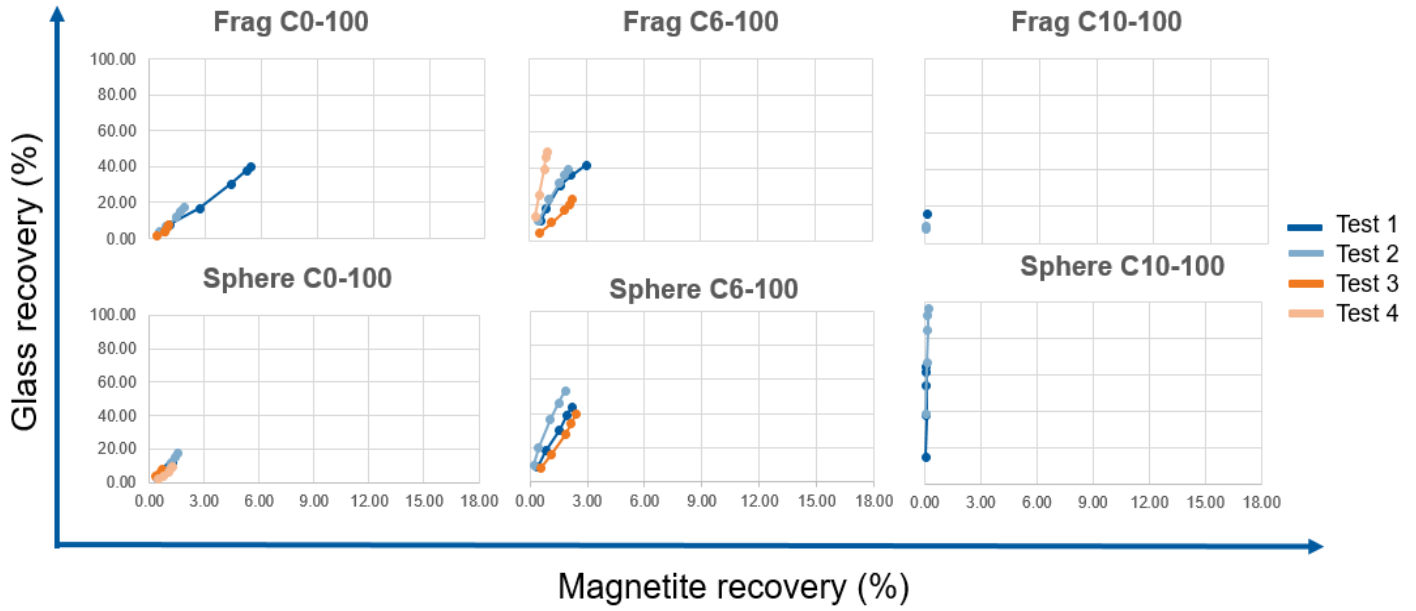

Appendix 20 Fuesrstenau upgrading curve of flotation test at 100 cm column

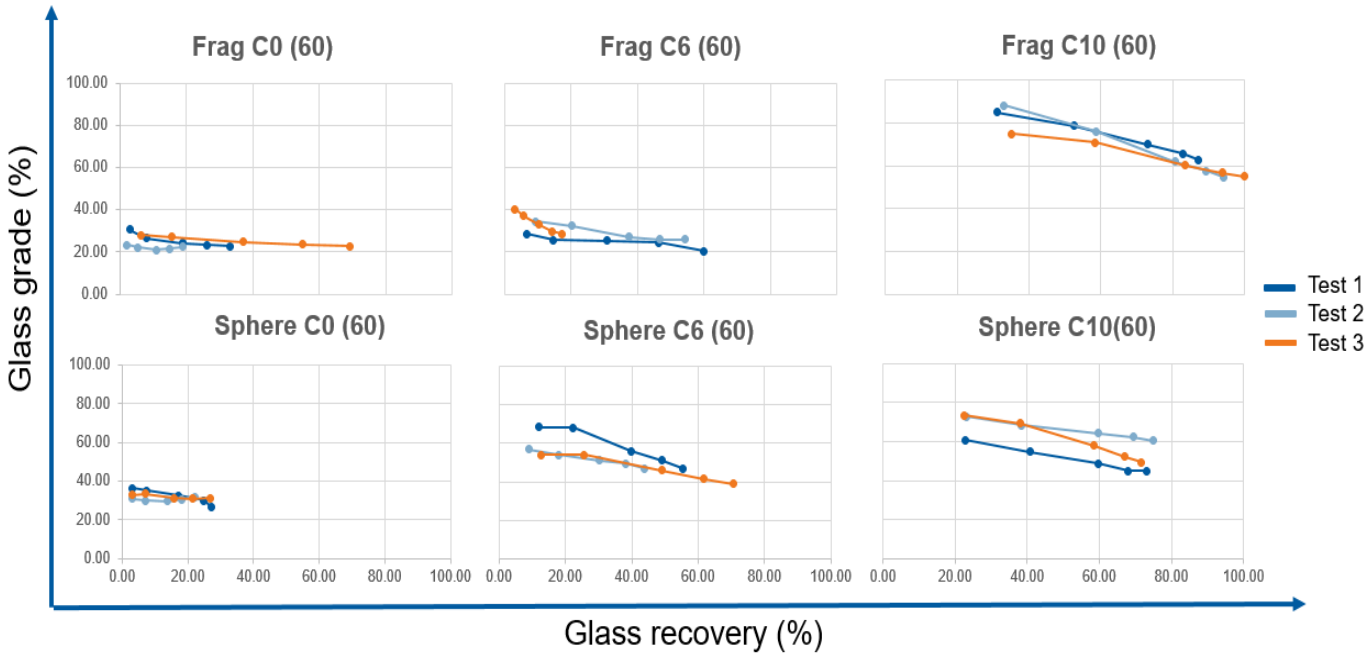

Appendix 21 HALBICH diagram – at 60 column

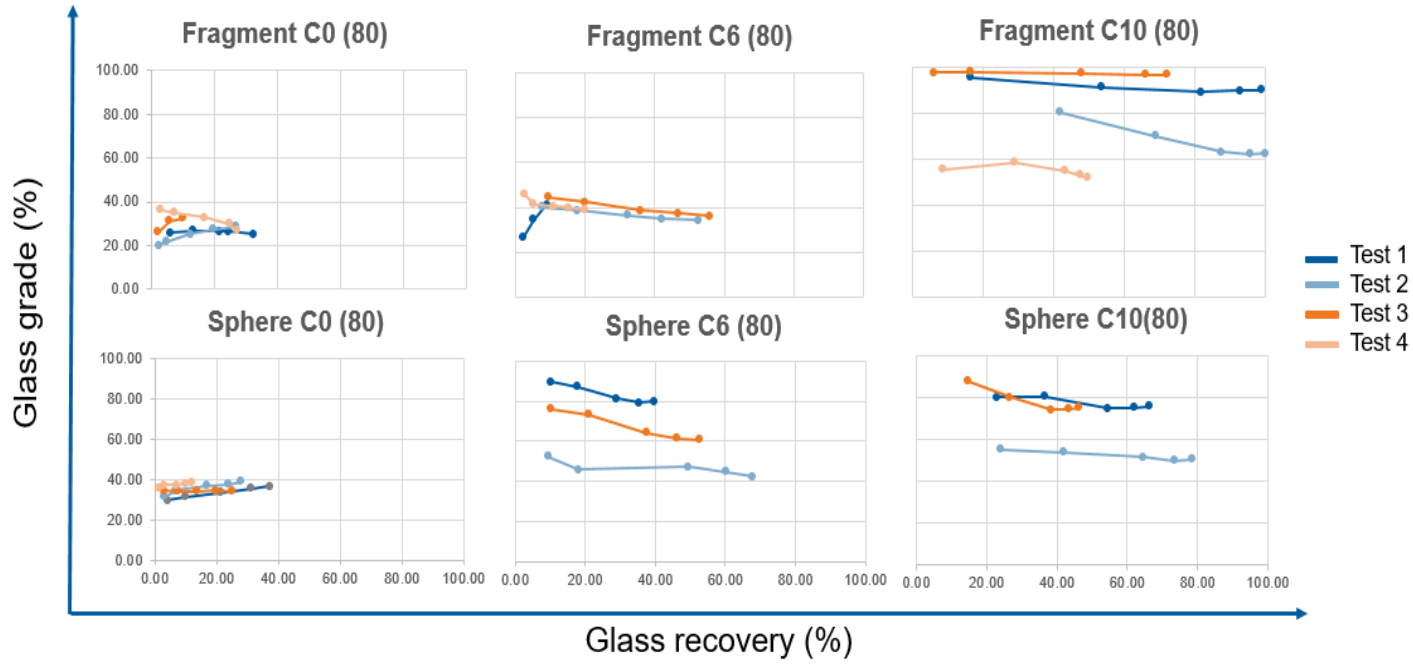

Appendix 22 HALBICH diagram – at 80 column

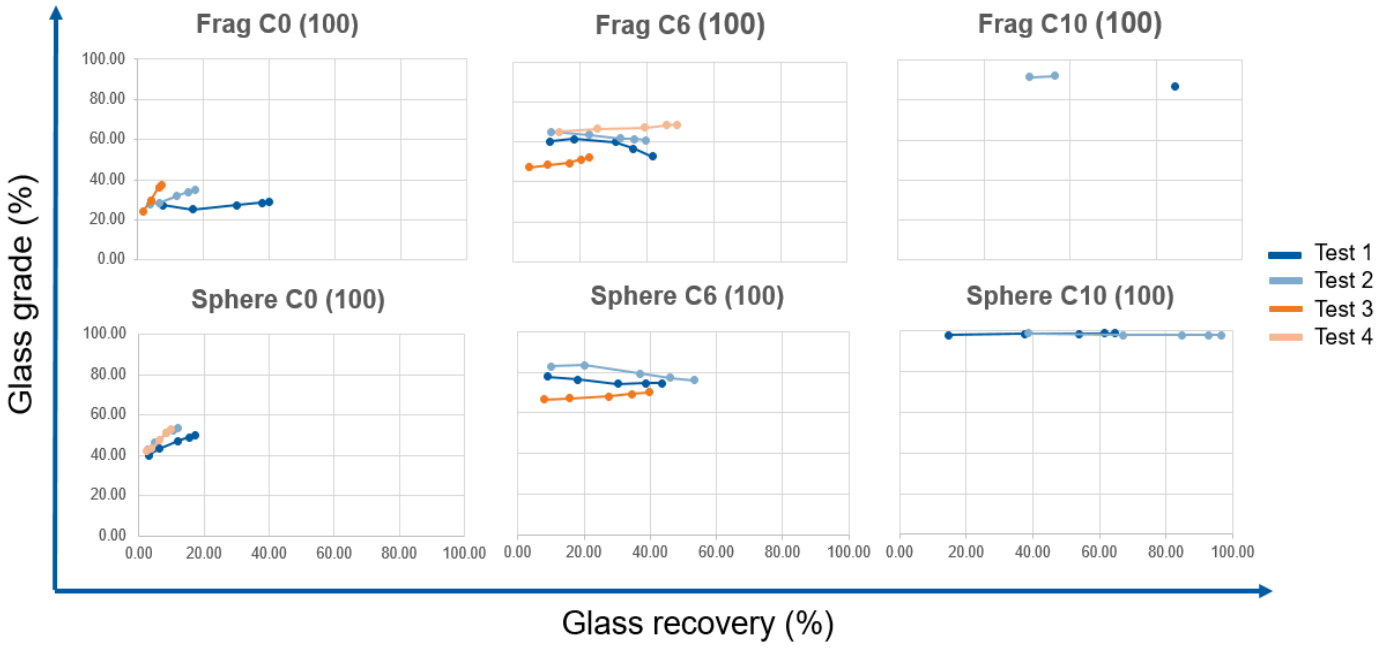

Appendix 23 HALBICH diagram – at 100 column